

Braid Equivalence in the Hénon Family I

A. de Carvalho T. Hall P. Hazard

March 5, 2022

Abstract

We give two general constructions of braid equivalences which exist between certain deformations of the 2-branched Horseshoe map. We then give numerical evidence suggesting that these constructions of braid equivalences are always realised in the Hénon family.

1 Introduction

During the last three decades of the twentieth century, much effort was devoted to the study of families of low-dimensional dynamical systems depending on parameters. There is today a very thorough theory explaining the dynamics of families of one-dimensional (real and complex) endomorphisms. The dynamics of the real quadratic family $f_a(x) = a - x^2$, for example, is nearly completely understood [12]. In the 1970s Hénon introduced the family¹ which now bears his name, a two-dimensional analog of the quadratic family: $F_{a,b}(x, y) = (f_a(x) - by, x)$. This is a family of plane diffeomorphisms depending on two parameters which, for $b = 0$, degenerates to the quadratic family. In contrast to the quadratic family, and despite the existence of several beautiful results about it, our understanding of the Hénon family is still rather rudimentary. While there are many similarities between the two families which make it possible to use knowledge of the former to help in understanding the latter, there are also many fundamental differences which demand that different techniques be developed.

One of the most basic aspects of the dynamics of a parametrized family is the way in which the periodic orbit structure changes as the parameters vary. This article is concerned with periodic orbits in Hénon family in the parameter regions close to degeneration, and exploits both similarities and differences between the quadratic and Hénon families.

¹Hénon considered a different parametrisation of this family,

$$H_{a,b}(x, y) = (-y + 1 - ax^2, bx)$$

Periodic orbits of endomorphisms of the real line are specified by their associated cyclic permutation: the way that their points, ordered on the line, are permuted by the endomorphism. For homeomorphisms of the plane such as Hénon maps, the analogous specification, introduced by Boyland [2, 3], is the braid type. If $F: \mathbb{R}^2 \rightarrow \mathbb{R}^2$ is an orientation-preserving homeomorphism and P is a periodic orbit of F , then the braid type $\text{bt}(P, F)$ is the isotopy class of F relative to P , up to topological conjugacy. In other words, the braid type of P is determined by fixing the action of F on P but allowing it to be deformed by isotopy in the complement of P , and also allowing a global change of coordinates.

The periodic orbit structure of maps in the quadratic family – or, indeed, of any unimodal map f – is easily understood using techniques of kneading theory. The critical point c is used to divide the line into left and right halves, and the kneading sequence of f is the itinerary of the critical value $f(c)$: the sequence of lefts and rights along the orbit $(f^n(c))_{n \geq 1}$. There is then a simple recipe for generating the set of all itineraries of points $x \in \mathbb{R}$ from this kneading sequence. Permutations associated to periodic orbits of unimodal maps – which are called *unimodal permutations* – are determined by the itineraries of the points on the orbit. The set of permutations of periodic orbits of a unimodal map f is therefore determined by the kneading sequence of the map, and can be enumerated by a straightforward algorithm.

The situation for the Hénon family is quite different. We have very little idea, to this day, of the way in which braid types of periodic orbits are built up in the family, going from none to a full horseshoe's worth, as the parameter a increases. In fact, by the result of Kan, Koçak and Yorke [11], periodic orbits of the Hénon family are both created and destroyed near every homoclinic tangency, and it is not even known whether or not all periodic orbits which appear in the Hénon family have the same braid type as periodic orbits of the horseshoe.

The diagrams in Figure 1 show regions in the parameter plane for the Hénon family where attracting periodic orbits of periods 8, 9, 10, and 11 were found. (Similar loci, for various periods, were first considered by El Hamouly and Mira [7].) These plots have a very rich structure, and understanding how the dynamics varies in the Hénon family includes explaining this structure. In this paper we are particularly interested in the hook-like structures, also called *swallow configurations* by Milnor [13] in the one-dimensional cubic case. These structures are open sets consisting of a main body and four limbs, two of which intersect the a -axis in two distinct (small) intervals. Each of these hooks indicates that there is one attracting periodic orbit in the Hénon family which can be deformed into two different attracting periodic orbits of the quadratic family. That is, we expect each of the hooks to be associated to attracting periodic orbits of the corresponding Hénon maps whose braid type is constant in the region $b > 0$ and which

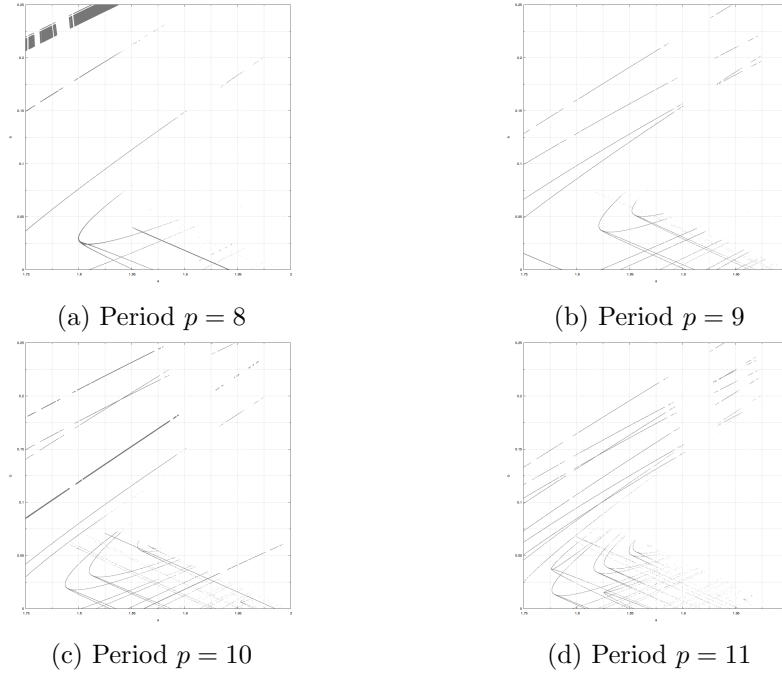


Figure 1: Scatterplots of parameters $(a, b) \in [1.75, 2.00] \times [0.0, 0.25]$ for which the Hénon map $F_{a,b}$ possesses an attracting periodic orbit of period $p = 8, 9, 10, 11$. One of the “hook-like” structures for period 8 can be seen intersecting the a -axis in two intervals at approximately $a = 1.8517$ and $a = 1.87$ respectively.

degenerate into periodic orbits of the quadratic family with two different permutations as $b \downarrow 0$ along each of the two ends of the hook. Viewing this in the opposite direction, the hooks indicate that there are certain pairs of unimodal permutations which coalesce into a single Hénon periodic orbit.

In this paper we identify mechanisms which lead to this coalescence on the level of unimodal permutations. More precisely, we describe two mechanisms which associate to unimodal permutations pairs of equivalent braids, and provide numerical evidence showing that the hooks in Figure 1 can all be explained in terms of these mechanisms.

There are at least two distinct reasons for which it is useful to be able to relate unimodal permutations to braid equivalences in the Hénon family. First, as mentioned above, our understanding of the periodic orbit structure of Hénon maps is very limited, and being able to connect Hénon braid types to unimodal permutations provides a means of deducing information about the former from the latter (about which we know everything); one of the consequences of our results is that we predict the existence of infinitely many hooks in the Hénon family, each of which associates a braid type with a pair of intervals in the parameter space of the quadratic family. Second, the

more general problem of deciding whether or not two braid types are equal is a difficult one, and mechanisms for constructing equivalent braids can be useful. For example, there are conjectural constraints [4] on the possible orders in which horseshoe braid types can be built up in families which pass from trivial dynamics to a full horseshoe; and if this conjecture holds, then each pair of equivalent braids generates an infinite family of pairs of equivalent braids.

We next review some definitions and terminology which will make it possible to give rough descriptions of the two mechanisms mentioned above. A geometric braid on n strands (see Figure 3) is a diagram with n arcs (strands) connecting two ordered sets of n points lined up vertically, so that only double intersections are allowed and at each of them it is specified which strand goes above and which goes below. The points at the top are called initial endpoints and those at the bottom are called terminal endpoints. To each geometric braid is associated a braid type, and braid types determine geometric braids up to conjugacy (these facts will be discussed further in the text). Geometric braids also induce permutations on n elements in the obvious way: associate to the initial endpoint the terminal endpoint along the same strand. Since this association forgets all information about crossings of strands, it is far from being one-to-one. It is possible, however, to associate a unique braid to a unimodal permutation by requiring that each pair of strands crosses at most once and that, when two strands cross, the one which started to the left goes above the one which started to the right. In this way we can talk about the unimodal braid associated with a unimodal permutation.

Given a unimodal permutation v , let f be a unimodal map realising v as its critical orbit. The *dynamical* preimage of a point in the critical orbit is the preimage under f which is also contained in the critical orbit (corresponding to the unique preimage at the level of the permutation). The other preimage of a point of the critical orbit is called the *non-dynamical* preimage.

The first mechanism is as follows. First we ‘break’ f at the dynamical preimage of the critical point: that is, we perturb f in a neighbourhood of this point. Assuming that the break is small, we get a new point which is a closest return to the critical point. Make this new point follow the sequence of forward iterates of the critical point: we may do this for any finite time by making the break sufficiently small. If we arrive near the non-dynamical preimage of the critical point, we can ‘reconnect’ this iterate of the new point to the critical point. Again, this means that we perturb f in a neighborhood of this iterate so that its image is the critical point. Depending on which side of the critical point the new point lies, we get a pair of distinct critical orbit types. (In terms of braids this construction is a generalisation of the cabling construction for a braid, followed by a half-twist between strands.)

The second mechanism takes a pair of equivalent unimodal permutations v_- and v_+ , such as those generated by the first mechanism, and produces another equivalent pair v_-^1 and v_+^1 of unimodal permutations. Let f_- and f_+ denote unimodal maps whose critical orbits realise v_- and v_+ respectively. As before, we break f_- and f_+ at the dynamical preimage, but in both cases the break is large so that the new point is a second closest return to the critical point. This is done to ensure that the image of the new point is close to the image of the first closest return. We make this image of the new point follow the forward iterates of the first closest return until it arrives close to the dynamical preimage of the critical point. It is then reconnected to the critical point as before. By repeating this process, a chain of pairs of equivalent braids can be generated.

In Section 2 we present some background on braids and unimodal maps; in Sections 3 and 4 the first and second constructions of braid equivalences are described; and in Section 5 we discuss applications to the Hénon family and numerical results.

Acknowledgements. A. de Carvalho was partially supported by FAPESP grant 2011/16265-8. T. Hall was partially supported by FAPESP grant 2011/17581-0. P. Hazard was supported by FAPESP grant 2008/10659-1 and Leverhulme Trust grant RPG-279. We would like to thank the institutions IME-USP, IMPA and the IMS at Stony Brook for their hospitality during the time in which parts of this work was done. Thanks also to A. Hammerlindl for his help with numerical computations. Finally, we would like to thank C. Tresser for useful discussions on braids and the Hénon family.

2 Notation and Terminology

2.1 Braids and Braid Equivalence

Let $\Delta \subset \mathbb{R}^2$ denote the closed unit disk. Let $\text{Homeo}_+(\Delta)$ denote the group of orientation-preserving homeomorphisms of Δ . Given a subset $A \subset \Delta$ let $\text{Homeo}_+(\Delta, A)$ denote the group of orientation-preserving homeomorphisms f of Δ satisfying $f(A) = A$. Where necessary we endow these groups with the uniform topology.

2.1.1 Braid Equivalence

Let $p \in \mathbb{N}$. Let $P_{\text{can}} \subset \Delta$ denote the unique set of p points contained in the horizontal axis, whose complement in this axis has connected components all of equal length. Let $F \in \text{Homeo}_+(\Delta, P_{\text{can}})$. Denote by $[F]_{P_{\text{can}}}$ the isotopy

class of F rel P_{can} . When it is clear from the context, we will also use the notation $[F]$.

The group of such isotopy classes under composition is called the *mapping class group* of (Δ, P_{can}) and is denoted by MCG_p .

Let $F \in \text{Homeo}_+(\Delta)$ possess a periodic orbit P of smallest period p . We assume P is in the interior of Δ : if not, we extend F arbitrarily over a collaring of Δ . Let $H: (\Delta, P_{\text{can}}) \rightarrow (\Delta, P)$ be any homeomorphism. Then the *braid type* of (P, F) is the conjugacy class $\langle [H^{-1} \circ F \circ H] \rangle$ of $[H^{-1} \circ F \circ H]$ in MCG_p . Denote the braid type of (P, F) by $\text{bt}(P, F)$. Let BT_p denote the set of all braid types of a fixed period p .

Remark 2.1. The braid type is independent of the collaring and the choice of homeomorphism H (see [8] for more details).

Let $F_0, F_1 \in \text{Homeo}_+(\Delta)$ possess periodic orbits P_0 and P_1 respectively. We say that the pair (P_0, F_0) and (P_1, F_1) are *braid equivalent* if $\text{bt}(P_0, F_0) = \text{bt}(P_1, F_1)$. Denote this equivalence by $(P_0, F_0) \sim_{BE} (P_1, F_1)$. Equivalently, $(P_0, F_0) \sim_{BE} (P_1, F_1)$ if there exists a homeomorphism $H: (\Delta, P_0) \rightarrow (\Delta, P_1)$ such that $F_0 \simeq H^{-1} \circ F_1 \circ H$ rel P_0 in Δ .

2.1.2 Braids

We now relate the notion of braid equivalence to that of a braid. Let B_p denote the braid group on p strands (see [1]). Denote the composition of braids $\alpha, \beta \in B_p$ by $\alpha \cdot \beta$. If α and β are *conjugate* we write $\alpha \sim \beta$. If α and β are *reverse-conjugate*, i.e. $\alpha \cdot \gamma = \gamma^{-1} \cdot \beta$ for some $\gamma \in B_p$, we write $\alpha \sim_r \beta$.

Remark 2.2. We will consider braids, geometric braids and braid diagrams. Typically we will not make the distinction. However, where necessary we will use the notation $a \simeq b$ to denote that the geometric braids a and b are isotopic. We will also denote their product by $a \cdot b$, whenever the set of terminal endpoints of b coincides with the set of initial endpoints of a .

Let $Z(B_p)$ denote the centre of B_p . It is known that $B_p/Z(B_p)$ is naturally isomorphic to MCG_p (see [9]). Hence BT_p is in one-to-one correspondence with the set of conjugacy classes of $B_p/Z(B_p)$ whose underlying permutation is a cycle (and hence close up to give a knot, rather than just a link). Therefore, given (P_F, F) we denote by $\beta(P_F, F)$ the conjugacy class in $B_p/Z(B_p)$ corresponding to $\text{bt}(P_F, F)$.

Remark 2.3. The following is well-known. Let (P_0, F_0) and (P_1, F_1) have associated braids β_0 and β_1 . Then $(P_0, F_0) \sim_{BE} (P_1, F_1)$ if and only if there exists a braid σ and $m \in \mathbb{Z}$ such that $\sigma^{-1} \cdot \beta_0 \cdot \sigma$ can be deformed into $\beta_1 \cdot \tau^m$ by a sequence of isotopies, 2nd and 3rd Reidemeister moves and their inverses, where τ is a braid associated to a generator of $Z(B_p)$.

Finally, we observe that if $F \in \overline{\text{Homeo}_+(\Delta)}$ possesses a periodic orbit P of smallest period p which corresponds to an isolated fixed point of non-zero index for the iterate F^p , then any small perturbation $F' \in \text{Homeo}_+(\Delta)$ will also possess a periodic orbit P' which is a continuation of P and of the same period. Therefore we can define $\text{bt}(P, F) = \text{bt}(P', F')$. Since having an isolated fixed point of non-zero index is an open property, this is well-defined.

2.1.3 Braid Equivalence in Families

Definition 2.4 (Braid equivalence in parametrised families). Let $k \in \mathbb{N}$. Let $B \subset \mathbb{R}^k$ be a contractible bounded open set. Let $F \in C(B, \overline{\text{Homeo}_+(\Delta)})$ be a k -parameter family of continuous self-maps. We will use the notation F_b for the map $F(b)$. Let $B^0 = \{b \in B : F_b \in \text{Homeo}_+(\Delta)\}$. Let $b_0, b_1 \in B$ satisfy the property that F_{b_0} and F_{b_1} have periodic orbits P_0 and P_1 respectively, both of smallest period p . Then (P_0, F_{b_0}) and (P_1, F_{b_1}) are *braid equivalent in the family F* if

1. there exists a collection of p pairwise distinct points

$$P(t) = \{P^1(t), P^2(t), \dots, P^p(t)\} \subset \Delta \quad (2.1)$$

where $P^i(t)$ varies continuously with $t \in [0, 1]$ for each $i = 1, 2, \dots, p$, such that $P_0 = P(0)$ and $P_1 = P(1)$;

2. there exists a path $\gamma: [0, 1] \rightarrow B$ such that $\gamma(0) = b_0, \gamma(1) = b_1$ and $P(t)$ is a periodic orbit for $F_{\gamma(t)}$, for each $t \in [0, 1]$.

(Observe, necessarily $P(t)$ must have smallest period p for $F_{\gamma(t)}$ as the $P^i(t)$ are distinct.) In other words, the one-parameter sub-family $F_{\gamma(t)}$ realises a strong Nielsen equivalence between (P_0, F_{b_0}) and (P_1, F_{b_1}) .

Remark 2.5. Braid equivalence in a parametrised family implies braid equivalence.

We will be specifically interested in the case when $b_0, b_1 \in B \setminus B^0$ and $\gamma(b_0, b_1) \subset \text{Homeo}_+(\Delta)$. (The motivating example will be that F denotes the family of Hénon maps and F_{b_0}, F_{b_1} will correspond to quadratic maps.)

2.1.4 Braids and Braid Diagrams

Recall that braids can be represented by braid diagrams. Braid diagrams will be normalised in the following way: They lie in the unit square $[-1, 1] \times [-1, 1]$. Each strand has an *initial endpoint* lying in $[-1, 1]^{\text{init}} = [-1, 1] \times \{1\}$. Each strand has a *terminal endpoint* lying in $[-1, 1]^{\text{term}} = [-1, 1] \times \{-1\}$. The vertical line through any initial endpoint contains a terminal endpoint (and vice versa). All crossings are transverse. Only double points are allowed. The strands are directed downwards. (The last condition ensures no

strand can ‘backtrack’.) Consequently, if α and β are braids with associated diagrams, then the braid diagram corresponding to the product $\alpha \cdot \beta$ is the braid formed by placing the diagram corresponding to β directly above the diagram corresponding to α and rescaling.

Remark 2.6. We adopt this convention as it coincides with the convention of composing maps or isotopies from the right. For example, if the isotopy F_t^α realises the braid α and the isotopy F_t^β realises the braid β then $F_t^\alpha \cdot F_t^\beta$ realises the braid $\alpha \cdot \beta$.

Let β be a braid diagram. Denote by S_β the set of strands. Denote by E_β^{init} the set of initial endpoints. We will denote the points in E_β^{init} , ordered from left to right, by $0^{\text{init}}, 1^{\text{init}}, \dots, (p-1)^{\text{init}}$. Similarly, denote by E_β^{term} the set of terminal endpoints. We will denote the points in E_β^{term} , ordered from left to right, by $0^{\text{term}}, 1^{\text{term}}, \dots, (p-1)^{\text{term}}$. We denote the strand emanating from i^{init} by $s_\beta(i)$. Let $\pi: [-1, 1]^2 \rightarrow [-1, 1]$ denote the projection to the first coordinate. Then by assumption $\pi(i^{\text{init}}) = \pi(i^{\text{term}})$ for all $i = 0, 1, \dots, p-1$.

Given a strand $s \in S_\beta$ let s^{init} and s^{term} denote its initial and terminal endpoints respectively. When it is clear which braid β is being considered we will drop β from our notation, so that $s_\beta(i)$ becomes $s(i)$, $s_\beta(i)^{\text{init}}$ becomes $s(i)^{\text{init}}$, and so on.

2.2 Unimodal Dynamics

2.2.1 Unimodal Permutations

Remark 2.7. In this section we consider only intervals in $\{0, 1, \dots, p-1\}$, e.g. for $i, j \in \{0, 1, \dots, p-1\}$ satisfying $i < j$ we let

$$[i, j] = \{k \in \{0, 1, \dots, p-1\} : i \leq k \leq j\} \quad (2.2)$$

Define (i, j) , $[i, j)$ and $(i, j]$ similarly. In later sections we may also assume they are embedded in \mathbb{R} but it will be clear from the context what is meant.

Definition 2.8. Let $p \in \mathbb{N}$. Endow the set $\{0, 1, \dots, p-1\}$ with its natural ordering. A permutation v of the set $\{0, 1, \dots, p-1\}$ is *unimodal* if there exists $m \in (0, p-1)$, such that

1. v is order-preserving on the interval $[0, m]$
2. v is order-reversing on the interval $[m, p-1]$

We call m the *folding point* of v . We denote the set of unimodal permutations on $\{0, 1, \dots, p-1\}$ by U_p . Let $U = \bigcup_{p \in \mathbb{N}} U_p$.

If a unimodal permutation v is cyclic then we can introduce the following, which we call *cyclic notation*: Define $\circ: \{0, 1, \dots, p-1\} \rightarrow \{0, 1, \dots, p-1\}$

by $o(v^i(m)) = i$ for $i = 0, 1, \dots, p-1$. Then we may uniquely represent v by $(o(0), o(1), o(2), \dots, o(p-1))$. Observe that o is a bijection. Hence we can recover v by setting $v(o^{-1}(i)) = o^{-1}(i+1 \bmod p)$.

Example 2.9. The cyclic unimodal permutation v of $\{0, 1, 2, 3, 4\}$ given by

$$v(0) = 1, v(1) = 3, v(2) = 4, v(3) = 2, v(4) = 0 \quad (2.3)$$

has folding point $m = 2$ and therefore $o(2) = 0$. Applying v iteratively gives

$$o(4) = 1, o(0) = 2, o(1) = 3, o(3) = 4 \quad (2.4)$$

In cyclic notation ² we write $(o(0), o(1), o(2), o(3), o(4)) = (\underline{2}, \underline{3}, \underline{0}, \underline{4}, \underline{1})$. (In other words, cyclic notation is just shorthand for the collection of inequalities $v^2(m) < v^3(m) < m < v^4(m) < v(m)$.)

Definition 2.10. Let $v \in U_p$ be cyclic. Let $q \in \{0, 1, \dots, p-1\}$. We call q a *right closest return time* to the folding point if $v^q(m) < m$ and the interval $(v^q(m), m)$ does not contain $v^r(m)$ for any integer r . Similarly, call q a *left closest return time* to the folding point if $m > v^q(m)$ and the interval $(m, v^q(m))$ does not contain $v^r(m)$ for any integer r . Finally, we call $q \in \{0, 1, \dots, p-1\}$ a *closest return time* to the folding point if the interval $(v^{q+1}(m), v(m))$ does not contain any point $v^r(m)$ for any integer r .

Note that a closest return time will either be a left or right closest return time.

Definition 2.11. Let $v \in U_p$. Let $i, j, k \in \{0, 1, \dots, p-1\}$, $i < j$. We say the closed interval $[i, j]$ *maps over* k if $k \in v[i, j]$ and *maps strictly over* k if $k \in v(i, j)$.

Remark 2.12. For each $k \in \{0, 1, \dots, p-1\}$, $k \neq 0$ or $p-1$, it is clear that there exists an interval mapping strictly over k . It is also clear that each interval mapping strictly over the folding point m contains at least one subinterval of shortest length which also maps strictly over m . (The interval $[v^{-1}(k) - 1, v^{-1}(k) + 1]$ maps strictly over k and no strict subinterval also satisfies this property.) In fact, there are at most two intervals mapping over k of shortest length.

Definition 2.13. Let $v \in U_p$. For each $k \in \{0, 1, \dots, p-1\}$ we call $v^{-1}(k)$ the *dynamical preimage* of k . If $k \neq 0, p-1$, the *interval containing the dynamical preimage of* k is the shortest closed interval mapping strictly over k which contains the dynamical preimage $v^{-1}(k)$ of k . If $k = 0$ or $p-1$,

²Note that we will use underlinings to distinguish representations, so $\underline{3}$ denotes the third point in the orbit of $\underline{1} = p-1$, but 3 denotes the third point from the left.

the interval containing the dynamical preimage of k is the shortest closed interval mapping over k which contains $v^{-1}(k)$.

The other shortest closed interval strictly mapping over k , when it exists, is called the *interval containing the non-dynamical preimage of k* .

Example 2.14. The unimodal cyclic permutation v of $\{0, 1, 2, 3\}$ given by

$$v(0) = 2, v(1) = 3, v(2) = 1, v(3) = 0 \quad (2.5)$$

(which in cyclic notation is given by $(\underline{2}, 0, \underline{3}, \underline{1})$) does not have an interval containing the non-dynamical preimage of the folding point $m = 1$. To see this, observe that 1 has dynamical preimage 2 lying in the right interval. The only non-empty subinterval of the left interval is the left interval itself, $[0, 1]$. This maps to the interval $[2, 3]$. As $[2, 3]$ doesn't contain the folding point, the unimodal permutation v does not have an interval containing the non-dynamical preimage of the folding point.

Definition 2.15. Let $v \in U_p$ be cyclic. Given $i, j \in \{0, 1, \dots, p-1\}$, denote by $\kappa = \kappa(i, j) > 0$ the smallest positive integer such that $j = v^\kappa(i)$. If $v^l(i) \neq m$ for all $0 \leq l < \kappa$, let

$$\rho(i, j) = \text{card}\{0 \leq l < \kappa : v^l(i) > m\} \quad (2.6)$$

Definition 2.16. Let $v \in U_p$ be cyclic. We say that v is *reconnectable at the dynamical preimage* if the following property holds: let $D = [d^-, d^+]$ denote the interval containing the dynamical preimage d of $\underline{0}$. Then either $\rho(\underline{1}, d^-)$ is odd or $\rho(\underline{1}, d^+)$ is even, or both.

We say that v is *reconnectable at the non-dynamical preimage* if the following properties hold:

1. *[Preimage condition]* The interval containing the non-dynamical preimage of m exists. Denote it by $E = [e^-, e^+]$.
2. *[Parity condition]* Either $\rho(\underline{1}, e^-)$ is odd or $\rho(\underline{1}, e^+)$ is even, or both.

Remark 2.17. It will become clear in what follows that this notion also makes sense for other points $k \in \{0, 1, \dots, p-1\}$, $k \neq m$. However, for simplicity we will only consider reconnections at the folding point.

Recall that we aim to construct braid-equivalent pairs of unimodal combinatorial types starting from a given unimodal combinatorial type. In what follows it will become clear that the construction we propose works precisely when the initial combinatorial type is reconnectable, either at the dynamical preimage or non-dynamical preimage.

Example 2.18. Given a cyclic unimodal permutation v , even if the interval containing the non-dynamical preimage of m exists it may not be reconnectable. For example consider, in cyclic notation, $(\underline{2}, \underline{7}, \underline{3}, \underline{8}, \underline{0}, \underline{5}, \underline{4}, \underline{9}, \underline{6}, \underline{1})$.



Figure 2: The two types of crossings used to construct braid diagrams.

The dynamical preimage $\underline{9}$ of the folding point $\underline{0}$ lies to the right of $\underline{0}$. The interval containing the non-dynamical preimage of $\underline{0}$ is $[\underline{7}, \underline{3}]$. To calculate $\rho(\underline{1}, \underline{3})$ we count the number of elements of $\{\underline{1}, \underline{2}\}$ lying to the right of $\underline{0}$, of which there is 1. Similarly there are 4 elements of $\{\underline{1}, \underline{2}, \underline{3}, \underline{4}, \underline{5}, \underline{6}\}$ lying to the right of $\underline{0}$. Hence $\rho(\underline{1}, \underline{3}) = 1$ and $\rho(\underline{1}, \underline{7}) = 4$. Since $\underline{7} < \underline{3}$ the parity condition isn't satisfied.

2.2.2 Unimodal Braids

We call a braid *positive* if each crossing is positive (see Figure 2). A braid is *direct* if each strand crosses any other strand at most once³. It is known that for any permutation $v \in U_p$ there is a unique positive, direct braid β which induces v . We call such braids *unimodal*. Denote the set of unimodal braids on p strands by UB_p . Let $UB = \bigcup_{p \in \mathbb{N}} UB_p$.

A unimodal braid β possesses a canonical braid diagram satisfying:

1. All strands initiated at m or to the left of m travel rightwardly.
2. All strands initiated at a point to the right of m travel rightwardly, touch the *folded line* $\pi^{-1}(p-1)$, then travel leftwardly.

We call strands satisfying Properties 1 and 2 *unimodal strands*. Henceforth we will identify a unimodal braid β with the corresponding canonical unimodal braid diagram. For example, the canonical unimodal braid diagram for the permutation $(\underline{2}, \underline{3}, \underline{0}, \underline{4}, \underline{1})$, is shown in Figure 3 below.

Let S be a collection of unimodal strands, not necessarily forming a braid, which are positive, direct and which contains a folding strand $s(\underline{0})$. Let s be a strand in S . The strand r *unimodally follows* s in S if

1. r is unimodal, r^{init} neighbours s^{init} , and r^{term} neighbours s^{term}
2. the collection $S \cup \{r\}$ is positive and direct
3. r has crossings of the following types

³ In the literature such braids are called permutation braids – however, it will be useful to have an adjective to describe this property, as in [8].

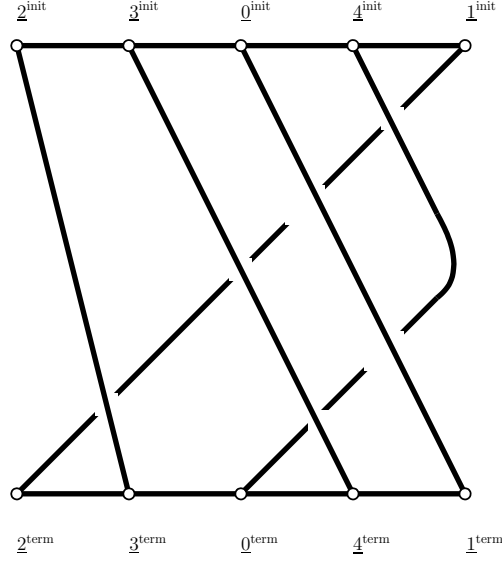


Figure 3: The braid β for the cyclic unimodal permutation $(\underline{2}, \underline{3}, \underline{0}, \underline{4}, \underline{1})$

- if t is a strand crossing s : then it also crosses r and the crossing is of the same type. All such crossings occur in the same order for r as they do for s .
- if s hits the folded line: then r hits the folded line and they cross once, when s is moving rightwardly but r is still moving leftwardly, or vice versa. Otherwise there is no crossing.

Let s and s' be strands in S such that $s^{\text{init}} < s'^{\text{init}}$ are neighbours lying on the same side of $\underline{0}$. A strand r *unimodally follows* the pair s, s' in S if

1. r is unimodal, r^{init} lies between s^{init} and s'^{init} , and r^{term} lies between s^{term} and s'^{term}
2. the collection $S \cup \{r\}$ is positive and direct.
3. r has crossings of three types
 - if t is a strand crossing both s and s' : then t makes the same type of crossing with r between its crossings with s' and s ;
 - if t is a strand crossing s' but not s : if r^{term} lies between s'^{term} and t^{term} , then r makes the same type of crossing with t after s' crosses t . Otherwise there is no crossing. Similarly, if t crosses s but not s' .
 - if s and s' hit the folded line, then r makes a single crossing both with s and with s' , either side of the single crossing between s and s' . Otherwise there are no crossings.

Before proceeding, let us make the following trivial observation concerning the action of half-twists on a cabled pair of strands.

Observation 2.19 (Fundamental Observation). Let β be a braid. Let s be a strand of β . Form a new strand s' which follows the strand s (i.e. makes the same crossings with all other strands and in the same order). Allow an arbitrary number of crossings between s and s' . Let β' denote the resulting braid⁴. Let τ_{init} denote a positive half-twist between s^{init} and s'^{init} . Let τ_{term} denote a positive half-twist between s^{term} and s'^{term} . Then $\beta' \cdot \tau_{\text{init}} = \tau_{\text{term}} \cdot \beta'$.

3 Breaking Braids Via First Closest Returns

3.1 Cabling

Our first construction extends that by Holmes [10] which generalised the cabling⁵ construction for iterated torus knots to horseshoe braids. Our description is in terms of braids rather than templates, but they are equivalent. Note that Holmes did not consider braid equivalence of the pairs of braids created by this construction. He considered only the single unimodal braid that resulted.

We now give an informal description of the cabling procedure. Given a cyclic braid $\beta \in B_p$, take the folding strand s_0 . ‘Break’ the braid by disconnecting s_0 from s_0^{term} and ‘glue’ it to a neighbouring point r_0^{term} which is not already the endpoint of some strand. Let r_1^{init} and s_1^{init} denote the vertical projection of r_0^{term} and s_0^{term} respectively. Let s_1 denote the strand emanating from s_1^{init} .

Add a strand r_1 with initial point r_1^{init} and which unimodally follows s_1 . Then r_1 has a terminal point r_1^{term} neighbouring s_1^{term} . Now repeat the process: Let r_2^{init} and s_2^{init} denote the vertical projection of r_1^{term} and s_1^{term} respectively. Add a strand r_2 unimodally following s_2 , etc.

The final strand r_{p-1} has initial point r_{p-1}^{init} and terminal point r_0^{term} . However, it may not be possible for r_{p-1} to follow s_{p-1} unimodally, as r_0^{term} may lie on the wrong side of s_0^{term} . Therefore r_{p-1} unimodally follows s_{p-1} until all other crossings have been made, then makes a negative crossing between s_{p-1} and r_{p-1} before connecting to r_0^{term} .

Given a unimodal braid β we can cable it in two distinct ways: to the left or right of the folding strand. It can be shown that this pair of braids are conjugate or reverse-conjugate. However, they are not both unimodal.

Observe that the cabling can be closed-up to form a braid whenever we land inside the interval containing the dynamical preimage of the folding point. More precisely, choose $q \in \mathbb{N}$ so that r_q^{term} lies in an interval

⁴Formally, these are not braids as they do not have the same set of initial and terminal endpoints. To avoid confusion, let us call these objects *almost-braids*.

⁵Although Holmes only used the term cabling for iterated torus knots (not iterated horseshoe knots) we will use the term for both cases.

$(s_q^{\text{term}}, s_{q'}^{\text{term}})$, not containing any terminal endpoints of β , and such that it maps over s_0^{term} . Let r_{q+1}^{init} denote the vertical projection of r_q^{term} . At this last step, construct a strand r_q emanating from r_q^{term} which, rather than completely following s_q , only follows s_q until we can reconnect r_q to s_0^{term} without creating any further crossings. We call this a *generalised cabling at the dynamical preimage*. Again there are two distinct cablings: to the left or right of the folding strand. As in the cabling case, the pair of braids are conjugate or reverse-conjugate. However, they are never both unimodal.

In Construction 3.1 below, we observe that the cabling can be closed-up at any point in time at which we lie in the interval containing the non-dynamical preimage of the folding point. We call this *generalised cabling at the non-dynamical preimage*. There are two preferred cablings, either side of the folding strand. Theorem 3.3 says this pair is conjugate or reverse-conjugate. What is important is that, unlike the previous two constructions, the braids produced by this process are both unimodal.

Construction 3.1 (Generalised Cabling – At the Non-Dynamical Preimage). Let $\beta \in UB_p$ be cyclic and reconnectable at the non-dynamical preimage. Let $v \in U_p$ denote the corresponding unimodal permutation. Let $E = [\underline{e}^-, \underline{e}^+]$ denote the interval containing the non-dynamical preimage of the folding point. Then either $\rho(\underline{1}, \underline{e}^-)$ is odd or $\rho(\underline{1}, \underline{e}^+)$ is even, or both. Let $\underline{q} - 1$ denote either of the points \underline{e}^- or \underline{e}^+ satisfying this parity condition.

Choose $\epsilon > 0$ small. Let $r_- \in (\underline{0} - \epsilon, \underline{0})$ and $r_+ \in (\underline{0}, \underline{0} + \epsilon)$. Let $r_1 \in (\underline{1} - \epsilon, \underline{1})$, $r_2 \in (\underline{2}, \underline{2} + \epsilon)$ and choose points $r_i \in (\underline{i} - \epsilon, \underline{i} + \epsilon)$, $i = 3, \dots, q-1$, which satisfy

$$r_i \in \begin{cases} (\underline{i} - \epsilon, \underline{i}) & \text{if } \rho(\underline{1}, \underline{i}) \text{ is even} \\ (\underline{i}, \underline{i} + \epsilon) & \text{if } \rho(\underline{1}, \underline{i}) \text{ is odd} \end{cases} \quad (3.1)$$

For $i = \pm 1, 2, \dots, q-1$, let r_i^{init} and r_i^{term} denote the projection of r_i to $[-1, 1]^{\text{init}}$ and $[-1, 1]^{\text{term}}$ respectively. These will be endpoints for the strands constructed below.

First, let $r_{\pm}(\underline{0})$ denote the strand with initial endpoint r_{\pm}^{init} and terminal endpoint r_1^{term} , which follows unimodally the strand $s(\underline{0})$.

Secondly, assume $r_{\pm}(\underline{i})$ have been constructed for $i = 0, \dots, j-1$, where $0 < j \leq q-2$. Let $r_+(j) = r_-(j)$ denote the strand with initial endpoint r_i^{init} and terminal endpoint r_{i+1}^{term} which follows unimodally the strand $s(\underline{i})$.

Thirdly, assume that the strands $r_{\pm}(\underline{i})$ have been constructed for all $i = 0, 1, \dots, q-2$. Construct the strand $r_{\pm}(\underline{q}-1)$ as follows. As $[\underline{e}^-, \underline{e}^+]$ maps over the folding point, one of the strands $s(\underline{e}^-)$ or $s(\underline{e}^+)$ has a terminal endpoint which lies on the same side of the folding point as its initial endpoint. Call it s and the other strand s' . Let $r_{\pm}(\underline{q}-1)$ denote the strand with initial endpoint r_{q-1}^{init} and terminal endpoint r_{\pm}^{term} which unimodally follows s and s' . We make modifications to $r_{\pm}(\underline{q}-1)$ as follows:

- (I) [If $\underline{0} < \underline{p}-1$.] Since $r_+^{\text{term}} > s(\underline{p}-1)^{\text{term}}$ and $r_{q-1}^{\text{init}} < \underline{0}^{\text{init}} < s(\underline{p}-1)^{\text{init}}$

we need an additional crossing between $r_+(q-1)$ and $s(p-1)$. Make a single *negative* crossing between $r_+(q-1)$ and $s(p-1)$ after all other crossings, resulting from $r_+(q-1)$ following s and s' , have been made.

Since $r_-^{\text{term}} < s(p-1)^{\text{term}}$ and $r_{q-1}^{\text{init}} < \underline{0}^{\text{init}} < s(p-1)^{\text{init}}$ no additional crossings between $r_-(q-1)$ and $s(p-1)$ are necessary.

- (II) [If $p-1 < \underline{0}$.] Since $r_-^{\text{term}} < s(p-1)^{\text{term}}$ and $s(p-1)^{\text{init}} < \underline{0}^{\text{init}} < r_{q-1}^{\text{init}}$ we need an additional crossing between $r_+(q-1)$ and $s(p-1)$. Make a single *negative* crossing between $r_+(q-1)$ and $s(p-1)$ after all other crossings, resulting from $r_+(q-1)$ following s , have been made.

Since $r_+^{\text{term}} > s(p-1)^{\text{term}}$ and $s(p-1)^{\text{init}} < \underline{0}^{\text{init}} < r_{q-1}^{\text{init}}$ no additional crossings between $r_+(q-1)$ and any other strand are necessary.

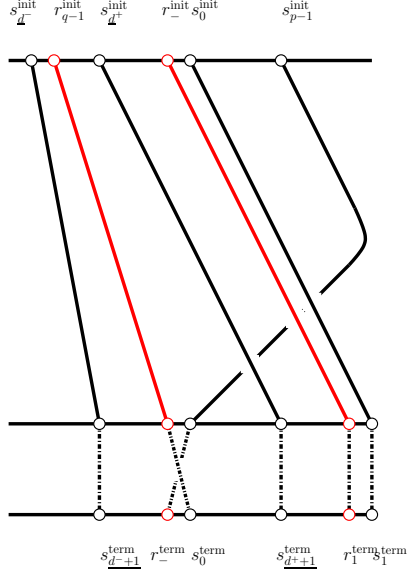
Let α_{\pm} denote the braid consisting of the strands of β , together with the strands $r_{\pm}(j), j = 0, 1, \dots, q-1$ formed above. Note that α_{\pm} is not cyclic. In fact, it is not necessarily unimodal. Let τ_{\pm} denote the positive half-twist between r_{\pm} and $\underline{0}$. (That is, τ_{\pm} is the Artin generator exchanging $\underline{0}$ and r_{\pm} via a single positive crossing.) Let $\beta_{\pm} = \tau_{\pm} \cdot \alpha_{\pm}$. Note that β_{\pm} is a cyclic braid. Moreover, after cancelling appropriate positive and negative crossings between the strands $r_{\pm}(q-1)$ and $s(p-1)$ via Reidemeister moves and isotopy, we see that, in both cases (I) and (II), that β_- and β_+ are unimodal.

Example 3.2. Consider the cyclic unimodal permutation v from Example 2.9. In cyclic notation it is given by $(\underline{2}, \underline{3}, \underline{0}, \underline{4}, \underline{1})$. Then the interval containing the non-dynamical preimage is $E = [\underline{2}, \underline{3}]$. Since $\rho(\underline{1}, \underline{2}) = 1$ is odd v is reconnectable at the nondynamical preimage. Let β denote the corresponding unimodal braid and β_{\pm} the pair of braids from Construction 3.1. If v_{\pm} denotes the permutation corresponding to β_{\pm} then

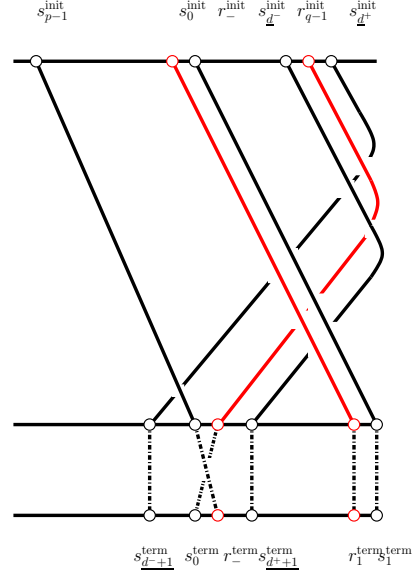
$$v_- = (\underline{2}, \underline{7}, \underline{3}, \underline{5}, \underline{0}, \underline{4}, \underline{6}, \underline{1}) \quad v_+ = (\underline{2}, \underline{7}, \underline{3}, \underline{0}, \underline{5}, \underline{4}, \underline{6}, \underline{1}) \quad (3.2)$$

See Figure 5 for the construction of β_{\pm} in this case.

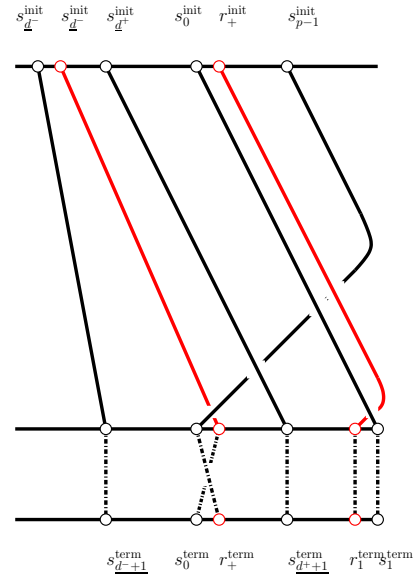
More generally, consider the case when the dynamical preimage of the folding point lies to the right of m . Then β_- and β_+ are depicted in Figures 4a and 4c respectively. Identifying the sets of initial and terminal endpoints of β_- and β_+ in an order-preserving manner, then precomposing β_- with a positive half-twist between the strand $s(\underline{0})$ and its neighbour r_- , and post-composing by the inverse of this twist, yields the braid β_+ . A similar argument can be given when the dynamical preimage of the folding point lies to the left of m . Then β_- and β_+ are shown in Figures 4b and 4d. However, in this case we precompose and post-compose by the same positive half-twist. Hence we have the following Theorem.



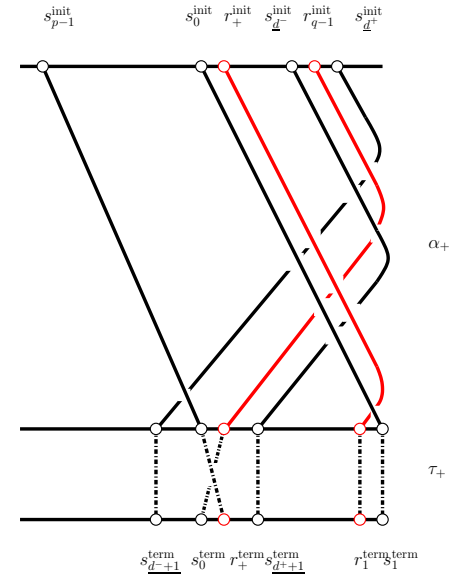
(a) β_- in Construction 3.1(I).



(b) β_- in Construction 3.1(II).

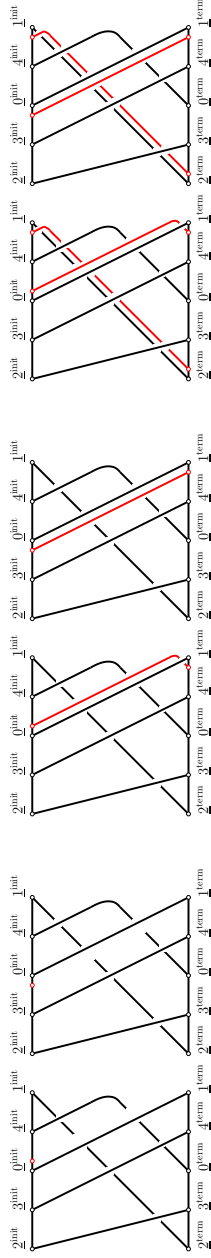


(c) β_+ in Construction 3.1(I).



(d) β_+ in Construction 3.1(II).

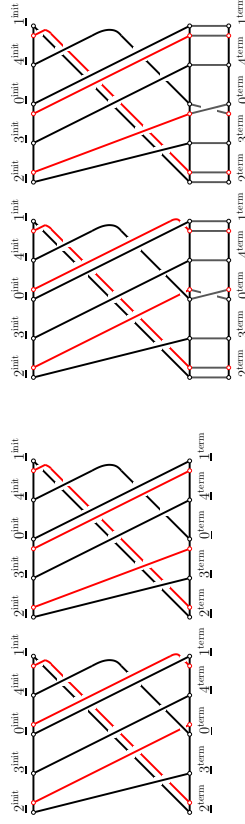
Figure 4: The braids β_- and β_+ from Construction 3.1. Only the necessary strands are shown. Strands from the original braid β are black, while new strands are red. (Only the first and last new strands are depicted.)



(a) Adding the first initial point r_{\pm}^{init} to β .

(b) Attaching the first strands $r_{\pm}(\underline{0})$.

(c) Attaching the second strands $r_{\pm}(\underline{1})$.



(d) Attaching the final strand $r_{\pm}(\underline{2})$.

(e) Performing the positive half-twist τ .

Figure 5: Adding strands to two copies of β from Example 3.2 resulting in the new braids β_- and β_+ .

Theorem 3.3. *Let $p \in \mathbb{N}$. Let $\beta \in UB_p$ be cyclic. Assume β is reconnectable at the non-dynamical preimage. Let β_- and β_+ denote the braids from Construction 3.1*

1. *If the non-dynamical preimage lies to the left of m then $\beta_+ \sim \beta_-$*
2. *If the non-dynamical preimage lies to the right of m then $\beta_+ \sim_r \beta_-$*

Theorem 3.3 and Remark 2.3 imply the following important corollary.

Corollary 3.4. *Let $p \in \mathbb{N}$. Let $v \in U_p$ be reconnectable at the non-dynamical preimage. Let v_- and v_+ denote the unimodal permutations from Construction 3.1.*

If $f_-, f_+ \in C([-1, 1], [-1, 1])$ are unimodal maps with periodic critical orbits C_- and C_+ of type v_- and v_+ respectively, then $(C_-, f_-) \sim_{BE} (C_+, f_+)$.

4 Breaking Braids Via Second Closest Returns

4.1 Generalised Cabling Process

We now describe a second construction that, given a braid-equivalent pair of unimodal permutations v_- and v_+ satisfying conditions given below, generates another pair of braid-equivalent unimodal permutations. Moreover, the new pair satisfy the same conditions and hence we can apply the construction once more. The idea is the following. Take v_{\pm} as given by Construction 3.1. Break the connection at 0^{term} and glue the free strand to a point just outside the interval $[p_-^{\text{term}}, p_+^{\text{term}}]$, making a *second closest return*. Then consecutively add strands, starting from this point, that unimodally follow the strands from initial endpoints $p_{\pm}^{\text{init}}, p_{\pm} + 1^{\text{init}}$, etc. Stop once a terminal endpoint lands inside D , the interval containing the dynamical preimage of the folding point. Finally, to close-up the braids, glue the last strand back to 0^{term} . However, since we will define the process inductively we need to enlarge the space of such pairs (not just those coming from Construction 3.1). Before giving the general construction, however, let us consider the following example.

Example 4.1. Let β_{\pm} denote the braids from Example 3.2. For notational clarity, let us initially denote the underlying permutations by

$$v_- = (\underline{2}_-, \underline{7}_-, \underline{3}_-, \underline{5}_-, \underline{0}_-, \underline{4}_-, \underline{6}_-, \underline{1}_-) \quad (4.1)$$

and

$$v_+ = (\underline{2}_+, \underline{7}_+, \underline{3}_+, \underline{0}_+, \underline{5}_+, \underline{4}_+, \underline{6}_+, \underline{1}_+) \quad (4.2)$$

The braids β_{\pm} are shown in Figure 7a. The initial and terminal endpoints of β_{\pm} are denoted by $0_{\pm}^{\text{init}}, 1_{\pm}^{\text{init}}, \dots, 7_{\pm}^{\text{init}}$ and $0_{\pm}^{\text{term}}, 1_{\pm}^{\text{term}}, \dots, 7_{\pm}^{\text{term}}$ respectively. Denote the corresponding strands by $s(0_{\pm}), \dots, s(7_{\pm})$. We may assume that

the endpoints of the strands in β_{\pm} have been moved, in an order-preserving manner, so that for all $k \neq 5$, $\underline{k}_{-}^{\text{init}} = \underline{k}_{+}^{\text{init}}$ and $\underline{k}_{-}^{\text{term}} = \underline{k}_{+}^{\text{term}}$. We may also assume that the strands have been deformed so that $s(\underline{k}_{-}) = s(\underline{k}_{+})$ for all $k \neq 4$ or 5 (i.e. any strand whose set of initial or terminal endpoints does not contain $\underline{5}_{\pm}^{\text{init}}$ or $\underline{5}_{\pm}^{\text{term}}$). Therefore, for all $k \neq 5$, denote the points $\underline{k}_{\pm}^{\text{init}}$ and $\underline{k}_{\pm}^{\text{term}}$ by $\underline{k}^{\text{init}}$ and $\underline{k}^{\text{term}}$ respectively. Similarly, for all $k \neq 4$ or 5 , denote the strands $s(\underline{k}_{\pm})$ simply by $s(\underline{k})$. See Figure 6. Let us do the following

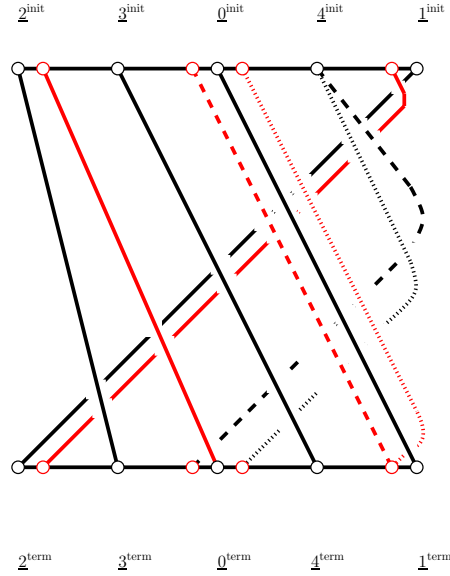
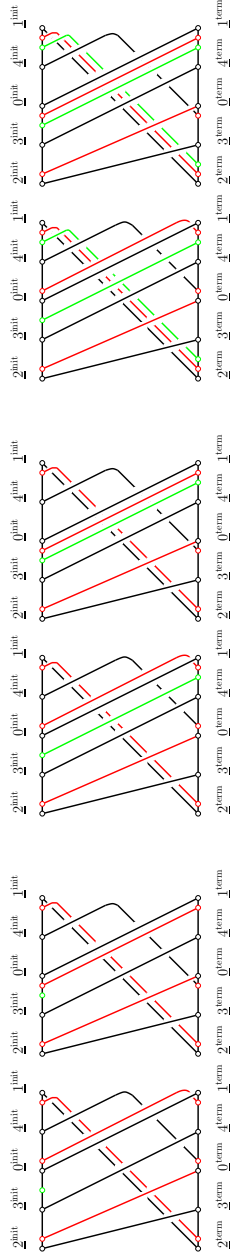


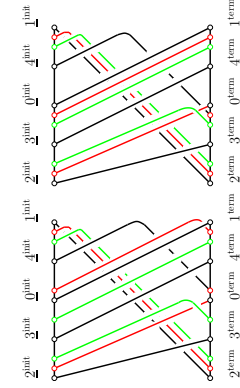
Figure 6: The braids β_{\pm} with strands in the same diagram, from Example 4.1. The strands with long dashes come from β_{-} , while the strands with short dashes come from β_{+} .

to the braids β_{-} and β_{+} . As shown in Figure 7a add an initial endpoint, shown in green, to the left of $\underline{5}_{-}^{\text{init}}$ in both diagrams. Add a strand, also shown in green, from this new initial endpoint which unimodally follows the strand $s(\underline{5}_{-})$. See Figure 7b. Next, add a new initial endpoint directly above the terminal endpoint of this last strand, which neighbours $\underline{6}^{\text{init}}$. From this initial endpoint add a new strand which unimodally follows the next strand $s(\underline{6})$. See Figure 7c. Observe that the new terminal endpoint lies inside the interval containing the dynamical preimage. Add a final initial endpoint directly above this terminal endpoint, necessarily neighbouring $\underline{7}^{\text{init}}$. From this initial endpoint add a strand which unimodally follows the strand $s(\underline{7})$ until $s(\underline{7})$ has made all its crossings *except* possibly for a single crossing with $s(\underline{4})$. Make the new strand form a negative crossing with the strand $s(\underline{7})$ before ending at a terminal endpoint directly below the very first initial endpoint we started with. See Figure 7d. This gives a pair of unimodal braids, which are non-cyclic (there are exactly two cycles). To form a pair of cyclic braids, perform a negative half-twist between this final terminal

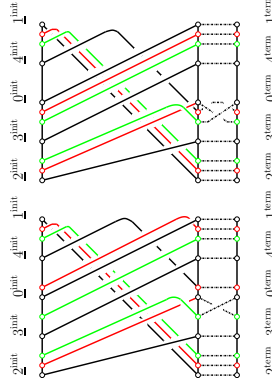


(a) Adding the first initial point.

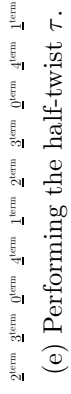
(b) Attaching the first strands.



(c) Attaching the second strands.



(d) Attaching the final strand.



(e) Performing the half-twist τ .

Figure 7: Adding strands to β_{\pm} from Example 3.2 resulting in the new braids β_{-}^1 and β_{+}^1 .

endpoint and $s(\underline{0})^{\text{term}}$. There is a complication in that for one of these braids, there is another terminal endpoint, namely $\underline{5}_+^{\text{term}}$, lying in between: we take the strand from this endpoint going *under* the half-twist. See Figure 7e. Denote the resulting braids by β_-^1 and β_+^1 . Conjugating β_+^1 by a positive half-twist between $\underline{0}$ and $\underline{5}_+$, the resulting braid can be deformed by a series of isotopies and Reidemeister moves into the braid β_+^1 .

Next, we need the following notions to simplify exposition. Given a unimodal permutation $v \in U_p$ and $\imath \in \{0, 1, \dots, p-1\}$, $\imath \neq \underline{0}$, we add a point $\bar{\imath}$ to the linearly ordered set $\{\underline{0}, \underline{1}, \dots, \underline{p-1}\}$, which we call the *opposite* of \imath with respect to v , which satisfies

- (i) $\bar{\imath} < \underline{0}$ if and only if $\imath > \underline{0}$
- (ii) $\bar{\imath} \in (\underline{j}, \underline{k})$ if and only if $v(\imath) \in (v(\underline{j}), v(\underline{k}))$.

Remark 4.2. Observe that, if the set $\{1, \dots, p-1\}$ is embedded in the line in an order-preserving manner and v is realised by a unimodal endomorphism f , then the opposite of a point \imath just corresponds to the preimage of $f(\imath)$ under f which is not \imath .

In what follows we only need to consider closest return times to the folding point, so we will simply say that p is the closest return time. (See Section 2.2 for the definition.)

For positive integers p and q , let $U_{p,q}$ denote the set of cyclic unimodal permutations of length $p+q$ with closest return time p . Given $v \in U_{p,q}$, let $C = [\underline{p}, \bar{p}]$, where \bar{p} denotes the opposite point of \underline{p} with respect to v . Let $D = [\underline{d}^-, \underline{d}^+]$ denote the interval containing the dynamical preimage $\underline{d} = p+q-1$ of $\underline{0}$. Let $D^- = [\underline{d}^-, \underline{d}]$ and $D^+ = [\underline{d}, \underline{d}^+]$. Let $E = [\underline{e}^-, \underline{e}^+]$ denote the interval containing the non-dynamical preimage.

Example 4.3. Observe that the unimodal permutations constructed in Example 3.2, and also considered in Example 4.1,

$$v_- = (2, \underline{7}, \underline{3}, \underline{5}_-, \underline{0}, \underline{4}, \underline{6}, \underline{1}), \text{ and } v_+ = (2, \underline{7}, \underline{3}, \underline{0}, \underline{5}_+, \underline{4}, \underline{6}, \underline{1}) \quad (4.3)$$

both lie in $U_{5,3}$, where we have kept the notation convention of Example 4.1. If we denote the intervals C, D, D^\pm, E for the permutation v_\pm by $C_\pm, D_\pm, D_\pm^\pm, E_\pm$, then we find that $C_- = [\underline{5}_-, \underline{5}_+] = C_+$, $D_- = [\underline{2}, \underline{3}] = D_+$, $D_-^- = [\underline{2}, \underline{7}] = D_+^-$, $D_-^+ = [\underline{7}, \underline{3}] = D_+^+$, $E_- = [\underline{0}, \underline{4}]$, and $E_+ = [\underline{4}, \underline{6}]$.

Now consider the general situation. Let $v_\pm \in U_{p,q}$. In cyclic notation denote v_\pm by $(\underline{2}_\pm, \dots, \underline{0}_\pm, \dots, \underline{1}_\pm)$. Assume the following:

1. (closest returns lie on opposite sides of the folding point) $\underline{p}_- < \underline{0}_-$ and $\underline{0}_+ < \underline{p}_+$.

2. (all remaining points are in order-preserving bijection) for all $k, l \neq p$, $\underline{k}_- < \underline{l}_-$ if and only if $\underline{k}_+ < \underline{l}_+$. Hence, if \underline{k}_\pm are embedded in the line in an order-preserving manner, as in the preceding example, we may assume that $\underline{k}_- = \underline{k}_+$ for all $k \neq p$. Consequently, for each $k \neq p$, we may denote the point \underline{k}_\pm by \underline{k} .
3. (the closest return is not contained in the interval containing the dynamical preimage of the folding point) $\underline{p}_\pm \notin \partial D_\pm$.
4. (the dynamical preimage of the folding point and the dynamical preimage of the closest return lie on opposite sides of the folding point) either $\underline{p+q-1}_\pm < \underline{0}_\pm < \underline{p-1}_\pm$, or $\underline{p-1}_\pm < \underline{0}_\pm < \underline{p+q-1}_\pm$.

Let $C_\pm, D_\pm, D_\pm^\pm, E_\pm$ denote the corresponding intervals for v_\pm . Then by (1) we may assume that $\underline{p}_- = \bar{p}_+$ and hence $C_- = C_+$. Denote this interval by C . Properties (2) and (3) then imply that $D_- = D_+$. Denote this interval by D . Similarly $D_-^\pm = D_+^\pm$ and we may denote this interval by D^\pm . Note that, as we saw in the previous Example 4.3, E_- and E_+ do not necessarily coincide.

By the discussion in Section 3, Condition (2) implies the following property, that will be used in the proof of Theorem 4.8 below.

- 2'. Let β_\pm denote the canonical unimodal braid of v_\pm . Then there exists a braid γ with $p+q$ strands, with the property that outside of $C = [\underline{p}_-, \underline{p}_+]$, γ is trivial, and such that one of the following holds:

$$\begin{aligned} 2'_+. \quad & \beta_- \cdot \gamma = \gamma \cdot \beta_+ \\ 2'_-. \quad & \beta_- \cdot \gamma = \gamma^{-1} \cdot \beta_+ \end{aligned}$$

Finally we will need the following trivial observation

5. (existence of the transit time from the closest return to the interval containing the dynamical preimage of the folding point) The orbit segment $\underline{p+1}, \underline{p+2}, \dots, \underline{p+q-1}$, of the image of the closest return point to the interval D does not intersect the interval C .

Call $t = q - 2$ the *transit time*. We say it is a *left transit time* if the parity, given by $\rho(\underline{p+1}, \underline{p+t+1})$, is even and a *right transit time* if this parity is odd.

Example 4.4. Let us continue consider v_\pm from Example 4.3. Then the transit time is $t = 1$, since $q = 3$. It is a right transit time. If we imagine a point neighbouring $\underline{p+1}$ to the left, then the image of that point lies in the interval containing the dynamical preimage, i.e. we land inside the interval containing the dynamical preimage after a single iterate. Moreover, this image lies to the right of the dynamical preimage of the folding point, therefore it is a right transit time.

Remark 4.5. Any pair (v_-, v_+) of equivalent unimodal permutations from Construction 3.1 satisfies properties (1)–(5). In particular, the unimodal permutations from Example 4.3 satisfy these conditions.

Construction 4.6 (Generalised Cabling Process.). Let (v_-, v_+) denote a pair of cyclic unimodal permutations satisfying properties (1)–(4). Recall that C_\pm, D_\pm , etc. denote the corresponding intervals for v_\pm . Recall that we may assume $C_- = C_+$ and $D_- = D_+$. Denote these intervals by C and D respectively. Observe that $v_-(D) = v_+(D)$ and this interval contains $\underline{0}$ and \underline{p}_\pm in its interior.

Let β_\pm denote the canonical braid corresponding to v_\pm . Denote the set of strands for β_\pm by S_\pm . For $k = 0, 1, \dots, p+q-1$, denote the k -th strand by $s_\pm(\underline{k})$. The strand $s_\pm(\underline{k})$ lies between initial endpoint $s_\pm(\underline{k})^{\text{init}} = \underline{k}_\pm^{\text{init}}$ and terminal endpoint $s_\pm(\underline{k})^{\text{term}} = \underline{k+1}_\pm^{\text{term}}$, where addition is taken modulo $p+q$. By property (4) above we may assume, after applying an isotopy if necessary, that $s_-(\underline{k}) = s_+(\underline{k})$ for all $k \neq p-1$ or p .

Remark 4.7. We will also use the notation s_k for the projection to $[-1, 1]$ of the initial endpoint of $s(\underline{k})$ for $k = 0, 1, \dots, p_-, p_+, \dots, p+q-1$.

Let t be the transit time. Construct a pair (v_-^1, v_+^1) of unimodal permutations as follows:

To begin, we define points r_i, r_i^{init} and r_i^{term} for $i = 0, 1, \dots, t+1$. Choose $\epsilon > 0$ small. Let $r_1 \in (\underline{p+1} - \epsilon, \underline{p+1})$, and choose points $r_i \in (\underline{p+i-1}, \underline{p+i+1})$, $i = 2, \dots, t+1$, which satisfy

$$r_i \in \begin{cases} (\underline{p+i-1}, \underline{p+i}) & \text{if } \rho(\underline{p+1}, \underline{p+i}) \text{ even} \\ (\underline{p+i}, \underline{p+i+1}) & \text{if } \rho(\underline{p+1}, \underline{p+i}) \text{ odd} \end{cases} \quad (4.4)$$

Finally, choose $r_0 \in (\underline{p_-} - 1, \underline{p_+} + 1)$ which satisfies

$$r_0 \in \begin{cases} (\underline{p_-} - \epsilon, \underline{p_-}) & \text{if } D < \underline{0} \text{ and } t \text{ a right time, or } \underline{0} < D \text{ and } t \text{ a left time.} \\ (\underline{p_+}, \underline{p_+} + \epsilon) & \text{if } D < \underline{0} \text{ and } t \text{ a left time, or } \underline{0} < D \text{ and } t \text{ a right time.} \end{cases} \quad (4.5)$$

For $i = 0, 1, 2, \dots, t+1$ let r_i^{init} and r_i^{term} denote the projections of r_i onto $[-1, 1]^{\text{init}}$ and $[-1, 1]^{\text{term}}$ respectively. As before, these will be endpoints for the strands constructed inductively below.

First, let $r_\pm(\underline{1})$ denote the strand with initial endpoint r_1^{init} and terminal endpoint r_2^{term} which follows unimodally the strand $s_\pm(\underline{p+1})$.

Secondly, assume that the strands $r_\pm(\underline{i})$ have been constructed for $i = 1, \dots, j-1$, for some $0 < j < t+1$. Let $r_\pm(\underline{j})$ denote the strand with initial endpoint r_j^{init} and terminal endpoint r_{j+1}^{term} which follows unimodally the strand $s_\pm(\underline{p+j})$.

Thirdly, assume that the strands $r_\pm(\underline{i})$ have been constructed for all $i = 1, 2, \dots, t$. Then $r_\pm(\underline{t+1})$ denotes the strand with initial endpoint r_{t+1}^{init} and terminal endpoint r_0^{term} which, in each of the four cases below, satisfies the following:

(Ii) [*If $p + q - 1 < 0$ and t is a left transit time.*]

Let $r_-(t+1)$ unimodally follow the strand $s_-(p+t+1)$ rightwardly until $s_-(p+t+1)$ has only one crossing to make, which is necessarily with $s_-(p-1)$, before reconnecting to its terminal endpoint. Then $r_-(t+1)$ forms a *negative* crossing with $s_-(p+t+1)$, after which it makes a *positive* crossing with $s_-(p-1)$ before connecting to its terminal endpoint. See Figure 8a.

Let $r_+(t+1)$ unimodally follow the strand $s_+(p+t+1)$ rightwardly until $s_+(p+t+1)$ has no more crossings to make before reconnecting to its terminal endpoint. Then $r_+(t+1)$ forms a *negative* crossing with $s_+(p+t+1)$, after which it makes a *positive* crossing with $s_+(p-1)$ before connecting to its terminal endpoint. See Figure 8c.

(Iii) [*If $p + q - 1 < 0$ and t a right transit time.*]

Let $r_-(t+1)$ unimodally follow the strand $s_-(p+t+1)$ rightwardly until $s_-(p+t+1)$ has only one crossing to make, which is necessarily with $s_-(p-1)$, before reconnecting to its terminal endpoint. Then $r_-(t+1)$ forms a *negative* crossing with $s_-(p+t+1)$ before connecting to its terminal endpoint. See Figure 8b.

Let $r_+(t+1)$ unimodally follow the strand $s_+(p+t+1)$ rightwardly until $s_+(p+t+1)$ has no further crossings to make before reconnecting to its terminal endpoint. Then $r_+(t+1)$ forms a *negative* crossing with $s_+(p+t+1)$ before connecting to its terminal endpoint. See Figure 8d.

(IIi) [*If $0 < p + q - 1$ and t a left transit time.*]

Let $r_-(t+1)$ unimodally follow $s_-(p+t+1)$ until $s_-(p+t+1)$ has no more crossings to make before reconnecting to its terminal endpoint. Then $r_-(t+1)$ forms a *negative* crossing with $s_-(p+t+1)$, after which it makes a *positive* crossing with $s_-(p-1)$ before connecting to its terminal endpoint. See Figure 9a.

Let $r_+(t+1)$ unimodally follow $s_+(p+t+1)$ until $s_+(p+t+1)$ has only one crossing to make, which is necessarily with $s_+(p-1)$, before reconnecting to its terminal endpoint. Then $r_+(t+1)$ forms a *positive* crossing with $s_+(p-1)$, after which it makes a *negative* crossing with $s_+(p+t+1)$ before connecting to its terminal endpoint. See Figure 9c.

(IIii) [*If $0 < p + q - 1$ and $t + 1$ a right transit time.*]

Let $r_-(t+1)$ unimodally follow $s_-(p+t+1)$ until $s_-(p+t+1)$ has no further crossings to make before connecting to its terminal endpoint. Then $r_-(t+1)$ forms a single *negative* crossing with $s_-(p+t+1)$ before connecting to its terminal endpoint. See Figure 9b.

Let $r_+(t+1)$ unimodally follow $s_+(p+t+1)$ until $s_+(p+t+1)$ has only one crossing to make, which is necessarily with $s_+(p-1)$, before connecting to its terminal endpoint. Then $r_+(t+1)$ forms a single *negative* crossing with $s_+(p+t+1)$ before connecting to its terminal endpoint. See Figure 9d.

Finally, let $r_\pm(0)$ denote the strand with initial endpoint r_0^{init} and terminal endpoint r_1^{term} which, in cases (Ii) and (IIi), follows unimodally the strand $s(p_-)$ and, in cases (Iii) and (IIi), follows unimodally the strand $s(p_-)$.

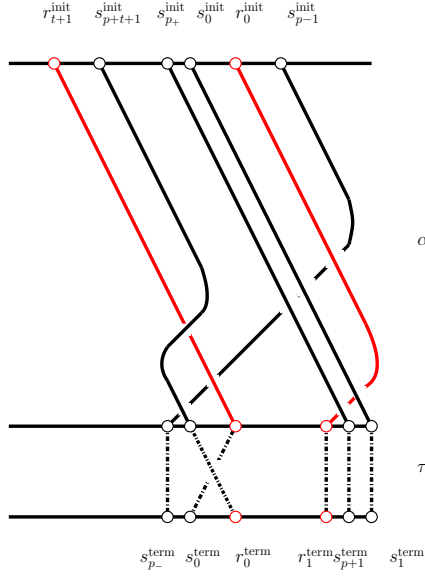
Let $\alpha_\pm^1 \in B_{p+q+t+2}$ denote the braid consisting of the strands of β_\pm together with the strands $r_\pm(i)$, $i = 0, 1, \dots, t+1$, formed above. (As before, after relabelling the endpoints this gives a well-defined braid diagram normalised as in Section 2.2.2. However, for the moment we will keep the labelling as above.) Note that α_\pm^1 is not a cyclic braid. Note also that α_\pm^1 is not necessarily a unimodal braid. In fact, in all cases α_\pm^1 is direct but neither positive nor unimodal. See Figures 8a–9d.

As in the previous construction, we now compose α_\pm^1 with a positive half-twist τ_\pm^1 . However, in terms of the diagram there is an extra complication due to either s_{p_-} or s_{p_+} lying between s_0 and r_0 . (Recall that, for each k , s_k denotes the projection to $[-1, 1]$ of the initial endpoint of $s(k)$.) Therefore let $\tau(i, i+1)$ denote the Artin generator positively interchanging i and $i+1$. Then

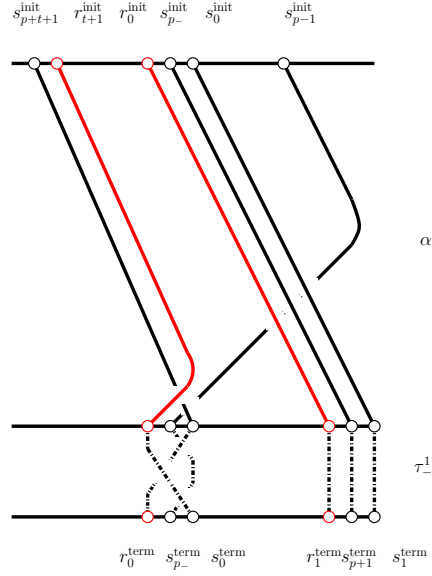
- (Ii) τ_-^1 denotes a single positive half-twist $\tau(s_0, r_0)$ between s_0 and r_0 .
 τ_+^1 denotes $\tau(s_0, s_{p_+})^{-1} \cdot \tau(s_{p_+}, r_0) \cdot \tau(s_0, s_{p_+})$.
- (Iii) τ_-^1 denotes $\tau(s_{p_-}, s_0) \cdot \tau(r_0, s_{p_-}) \cdot \tau(s_{p_-}, s_0)^{-1}$.
 τ_+^1 denotes a single positive half-twist $\tau(r_0, s_0)$ between r_0 and s_0 .
- (IIi) τ_-^1 denotes $\tau(s_{p_-}, s_0)^{-1} \cdot \tau(r_0, s_{p_-}) \cdot \tau(s_{p_-}, s_0)$.
 τ_+^1 denotes a single positive half-twist $\tau(r_0, s_0)$ between r_0 and s_0 .
- (IIii) τ_-^1 denotes a single positive half-twist $\tau(s_0, r_0)$ between s_0 and r_0 .
 τ_+^1 denotes $\tau(s_{p_+}, r_0)^{-1} \cdot \tau(s_0, s_{p_+}) \cdot \tau(s_{p_+}, r_0)$

Let $\beta_\pm^1 = \tau_\pm^1 \cdot \alpha_\pm^1$. Note that β_\pm^1 is a cyclic braid. Moreover, after cancelling appropriate crossings between strands $r_\pm(t+1)$, $s_\pm(p+t+1)$ and $s_\pm(p-1)$ via Reidemeister moves and isotopy, we find that β_-^1 and β_+^1 are both unimodal. Again, see Figures 8a–9d.

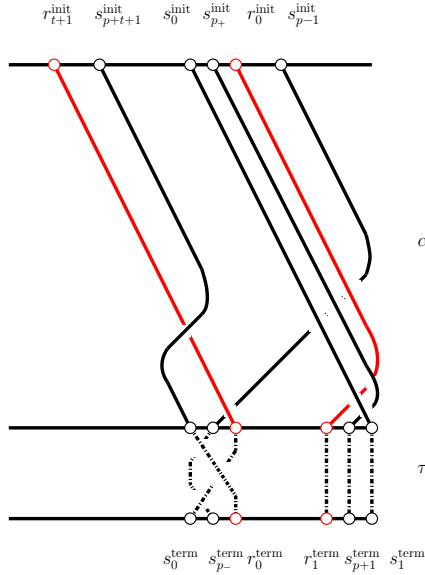
Let us investigate what is going on in more detail. Consider the case (Ii). Then β_- and β_+ are depicted in Figures 8a and 8c respectively. Identifying the sets of initial and terminal endpoints of β_- and β_+ in an order-preserving manner, then precomposing β_- with a positive half-twist between the strand $s(0)$ and its neighbour $s(p_-)$, and post-composing by the inverse of this twist,



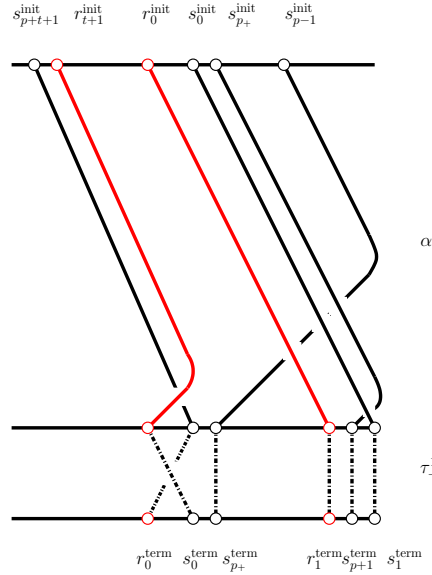
(a) β_- in Construction 4.6(Ii).



(b) β_- in Construction 4.6(Iii).

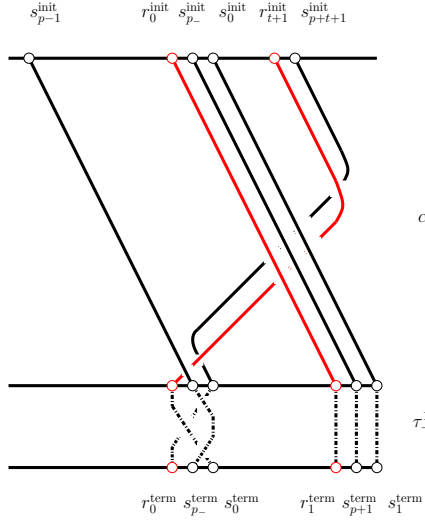


(c) β_+ in Construction 4.6(Ii).

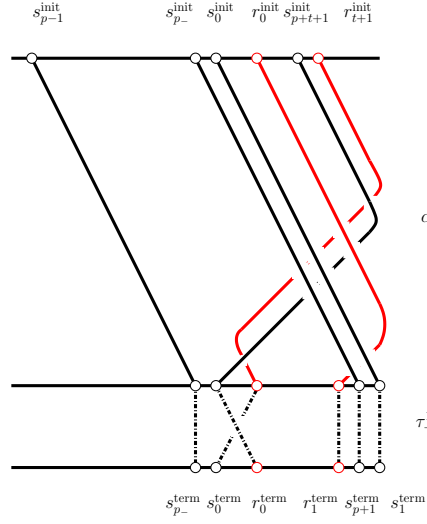


(d) β_+ in Construction 4.6(Iii).

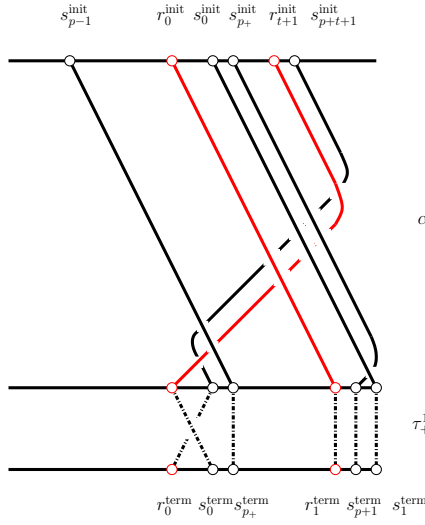
Figure 8: β_- and β_+ in Construction 4.6(I).



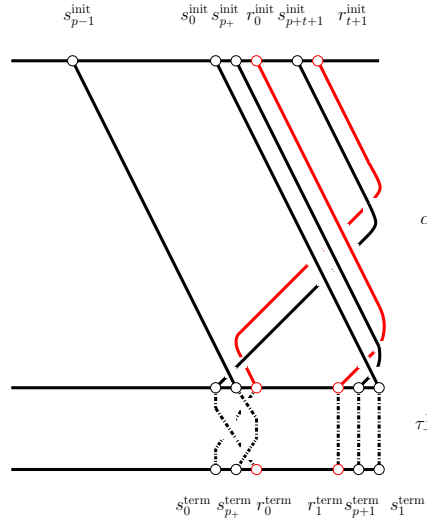
(a) β_- in Construction 4.6(III).



(b) β_- in Construction 4.6(III).



(c) β_+ in Construction 4.6(III).



(d) β_+ in Construction 4.6(III).

Figure 9: β_- and β_+ in construction 4.6(II).

yields the braid β_+ . A similar argument can be given in cases (Iii)–(IIii). See Figures 8b– 9d. However, in cases (IIi) and (IIii) we pre-compose and post-compose by the same positive half-twist. Hence we have the following.

Theorem 4.8. *Given (v_-, v_+) , satisfying properties (1)–(4). Let β_- and β_+ denote the corresponding unimodal braids. Let (β_-^1, β_+^1) denote the pair of braids produced from Construction 4.6.*

1. *If $\beta_- \sim \beta_+$ then $\beta_-^1 \sim \beta_+^1$.*
2. *If $\beta_- \sim_r \beta_+$ then $\beta_-^1 \sim_r \beta_+^1$.*

Moreover, the corresponding unimodal permutations (v_-^1, v_+^1) also satisfy the properties (1)–(4).

5 Applications to the Hénon Family

We have constructed two mechanisms for constructing braid equivalences. However, we would like to restrict ourselves to equivalences realised in the Hénon family.

Before proceeding, let us give a brief description of the parameter space of the quadratic family and the Hénon family. Recall from the introduction that $f_a(x) = a - x^2$ denotes the quadratic family and $F_{a,b}(x, y) = (a - x^2 - by, x)$ denotes the Hénon family. In the (a, b) -plane, for b positive the map $F_{a,b}$ is an orientation-preserving diffeomorphism. For $b \in (0, 1)$ the map $F_{a,b}$ is area-contracting. In fact, $\text{Jac}(F_{a,b})(x, y) = b$ for all $(a, b) \in \mathbb{R}^2$ and $(x, y) \in \mathbb{R}^2$.

The parabola

$$(1 + b)^2 + 4a = 0 \tag{5.1}$$

is the saddle-node bifurcation locus. For all parameters (a, b) on this curve $F_{a,b}$ possesses a unique fixed point. The parabola passes through the a -axis at $a = -1/4$. All parameters to the left of this curve possess no fixed point and the iterates of all points escape to infinity. All parameters to the right of the curve possess two fixed points, one saddle and one sink, and hence the non-wandering set is non-trivial.

The curve

$$a = (5 + 2\sqrt{5})(1 + b)^2 \tag{5.2}$$

lies to the right of the saddle-node bifurcation curve above. It was shown by Devaney-Nitecki [6] that for all parameters (a, b) lying to the right of this curve the map $F_{a,b}$ possesses a full horseshoe, and all points either escape to infinity or converge to this invariant set under iteration.

For a fixed b sufficiently small, increasing a from the saddle-node bifurcation locus to the horseshoe locus the map $F_{a,b}$ undergoes a period-doubling cascade. Each period-doubling bifurcation curve is algebraic and

they accumulate upon an analytic curve which intersects the a -axis at the Feigenbaum-Collet-Tresser parameter $a = 1.401\dots$. For parameters to the left of the accumulation of period-doubling, the map $F_{a,b}$ has simple dynamics: there are finitely many periodic orbits each of period 2^n for some non-negative integer n .

After this accumulation of period-doubling less is known. However, restricting to the a -axis we know more. Here between the accumulation of period-doubling and the horseshoe locus, uncountably many bifurcations occur. For each periodic kneading sequence there corresponds a hyperbolic component, i.e. an interval such that for each parameter in this interval $F_{a,b}$ has a periodic attractor whose itinerary is determined by the given periodic kneading sequence. For example, there is an interval around the point $a = 1.7549\dots$, for which every parameter has an attractive cycle of period three. (This parameter is actually the critically-periodic parameter, or centre, of the unique period-three hyperbolic component.)

These hyperbolic intervals extend to open subsets of the (a, b) -plane, where the periodic attractor persists. The loci of all such parameters, for fixed periods, were first considered by El-Hamouly and Mira [7]. Many components of this locus have the following structure: there exists a main ‘body’ out of which four ‘limbs’ emanate. Then limbs do not intersect; the union of the limbs and body is simply connected; two of the limbs intersect $\{b = 1\}$; the two remaining limbs intersect $\{b = 0\}$. (Similar configurations have been observed for the one-dimensional cubic family. These configurations have been called *swallow configurations* by Milnor [13].) Numerical investigations into the braid-equivalences exhibited in the (a, b) -plane were carried out by Holmes [10]. (See also Sannami [15].) However, currently very little is understood about these configurations. Their apparent prevalence, in the chaotic parameter region for the Hénon family as well as in other families, also requires explanation.

Remark 5.1. The braid equivalences we constructed were based on the initial unimodal permutation v possessing a non-dynamical preimage. This can only be satisfied if the corresponding kneading sequence satisfies $\kappa \succ 10C$ or, equivalently, has hyperbolic parameter interval lying to the right of the period-three hyperbolic parameter interval. Consequently, all numerical example given below intersect the a -axis in the interval $[1.7549\dots, 2]$. However, in [5] we will describe a generalisation of the construction of braid equivalences given here which do not have this restriction.

Following the numerical evidence given below, we ask the following questions. Let v_- and v_+ be an arbitrary pair of combinatorial types from Construction 3.1.

Question A. Let $a_-, a_+ \in [-1/4, 2]$ be such that f_{a_-} and f_{a_+} have critical orbits c_- and c_+ of types v_- and v_+ respectively. Let C_- and C_+ denote the corresponding periodic orbits for $F_{a_-,0}$

and $F_{a_+,0}$ respectively. Does there exist a braid equivalence in the family $F_{a,b}$ connecting $(C_-, F_{a_-,0})$ and $(C_+, F_{a_+,0})$?

The above question only deal with braid equivalences coming from Construction 3.1. Now, given an initial braid equivalent pair (v_-^0, v_+^0) , let us consider a sequence of equivalent pairs (v_-^i, v_+^i) coming from Construction 4.6.

Question B. For each positive integer i , let $a_-^i, a_+^i \in [-1/4, 2]$ be parameters such that $f_{a_-^i}$ and $f_{a_+^i}$ have critical orbits c_-^i and c_+^i of types v_-^i and v_+^i respectively. Let C_-^i and C_+^i denote the corresponding periodic orbits for $F_{a_-^i,0}$ and $F_{a_+^i,0}$ respectively. Does there exist, for each i , a braid equivalence in the family $F_{a,b}$ connecting $(C_-^i, F_{a_-^i,0})$ and $(C_+^i, F_{a_+^i,0})$? Are the paths γ^i in the (a, b) -plane which realise these braid equivalences pairwise disjoint?

We now give numerical evidence suggesting A and B are true. For simplicity we represent unimodal combinatorial types by the itinerary of the critical point (with respect to the standard partition $I_0 = [0, m)$, $I_C = m$, $I_1 = (m, p - 1]$.) Figures 1a– 1d showed plots of parameters for which $F_{a,b}$ possessed an attracting periodic orbit of a fixed period p . These regions connected distinct degenerate Hénon parameters. Numerically we construct a curve between such parameters as follows. First, take a unimodal permutation v satisfying the hypotheses of Construction 3.1, i.e. it is reconnectable at the non-dynamical preimage, and the non-dynamical preimage lies to the left of the folding point. Call v the *head*. Apply Construction 3.1, giving a braid-equivalent pair v_-^0 and v_+^0 . Then apply Construction 4.6 inductively, giving braid-equivalent pairs v_-^i and v_+^i for $i = 1, 2, 3$. This was repeated for various v . See Table 1 for orbits listed by itinerary and grouped by head, with the associated permutation given in cyclic notation. They are listed in pairs obtained as just described: the first pair is obtained from the head by Construction 3.1 and subsequent ones from Construction 4.6, inductively.

For each pair v_-^i and v_+^i we computed the superattracting parameters a_- and a_+ in the quadratic family with critical orbit of type v_- and v_+ respectively. Then the parameter locus of

$$F_{a,b}^p(x_{\text{in}}, y_{\text{in}}) = (x_{\text{in}}, y_{\text{in}}), \quad \text{tr} DF_{a,b}^p(x_{\text{in}}, y_{\text{in}}) = 0. \quad (5.3)$$

passing through the parameters $(a_-, 0)$ and $(a_+, 0)$ was computed. We call a parameter curve lying in the locus (5.3) a *zero isotracal path*. (More generally an *isotracal path* satisfies (5.3), but with the trace set to some fixed constant instead of zero.) We compute an isotracal curve iteratively by starting from the initial data given by

$$a = a_{\pm}, \quad b = 0, \quad x_{\text{in}} = a_{\pm}, \quad y_{\text{in}} = 0 \quad (5.4)$$

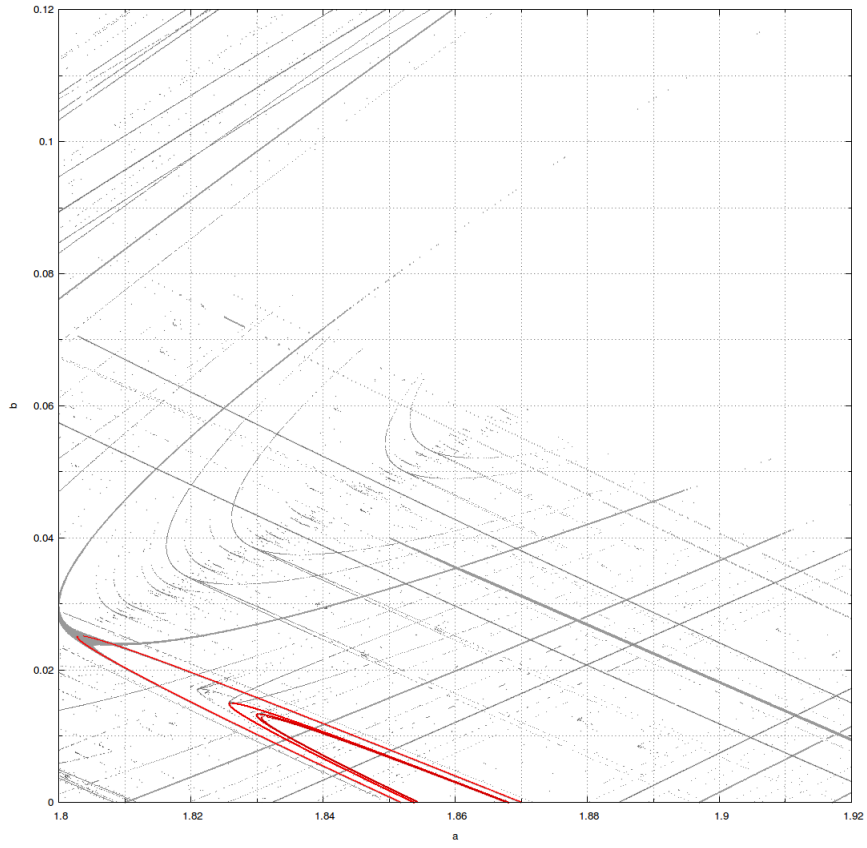


Figure 10: The isotracal curves of periods 8, 11, 14 and 17 generated from head 1001C are shown in red. The grey region show the scatterplots for periods 8, 11, 14 and 17. The darker the colour, the higher the period.

On each slice $\{b = b_0\}$, Newton's method was used to find $a = a(b_0)$, $x_{\text{in}} = x_{\text{in}}(b_0)$ and $y_{\text{in}} = y_{\text{in}}(b_0)$ satisfying equation (5.3). The value of b was then incremented and the values of a , x_{in} and y_{in} from the previous step were used as initial data. The algorithm terminated once $a_-(b)$ and $a_+(b)$ were sufficiently close.

Table 2 shows some of the braid equivalences which were realised in the Hénon family. The paths in the parameter region of $(a, b) \in [1.8, 1.9] \times [0.0, 0.1]$ are shown in Figure 11a. The red curves show the period 8, 11, 14 and 17 curves associated with head 1001C given in Table 2. They are shaded so that the darker the curve is, the higher the period. Similarly, the green curves show the period 9, 12, 15 and 18 curves associated with the head 10011C from Table 2. The blue curves show the period 10, 13, 16 and 19 curves associated with the head 100111C from Table 2. The yellow curves show the period 11, 14, 17 and 20 curves associated with the head 1001111C from Table 2. In each of these cases, the darker the curve is, the higher the period.

These plots were then superimposed with the scatterplots in Figures 10-11d. The grey region denoting the data from the first algorithm. So, for example, Figure 10 shows the curves of period 8, 11, 14 and 17 in Figure 11a together with the scatterplot data from the introduction for periods 8, 11, 14, and 17, where the darker the grey is the lower the period. Figures 11b and 11c are similar.

Table 2 also gives the prefix and decoration to compare the current mechanism with that given by the first and second authors (see [4] for more details on prefixes and decorations). For example consider the kneading sequences 10011110C and 10011010C (see Table 2). These have the same prefix 1001 but different decorations, 110 and 010 respectively, showing that braid equivalent sequences constructed by the mechanism in this article may have different decorations.

We can weaken Questions A and B by asking if these braid equivalences are realisable in a more general class of maps containing the Hénon family. The typical generalisation of the Hénon family is that of *Hénon-like maps*. These are maps of the form

$$F(x, y) = (f(x) - \varepsilon(x, y), x) \quad (5.5)$$

where f is unimodal on some interval J and $\varepsilon: J \times J \rightarrow \mathbb{R}$ satisfies $\partial_y \varepsilon > 0$. These are diffeomorphisms onto their images which appear, after a suitable change of variables, when considering maps in the neighbourhood of a homoclinic bifurcation [14].

Question A'. Given unimodal maps f_- and f_+ of type v_- and v_+ respectively, does there exist a family F_t , $t \in [-1, 1]$, of Hénon-like diffeomorphisms such that $F_{-1} = \iota(f_-)$ and $F_{+1} = \iota(f_+)$,

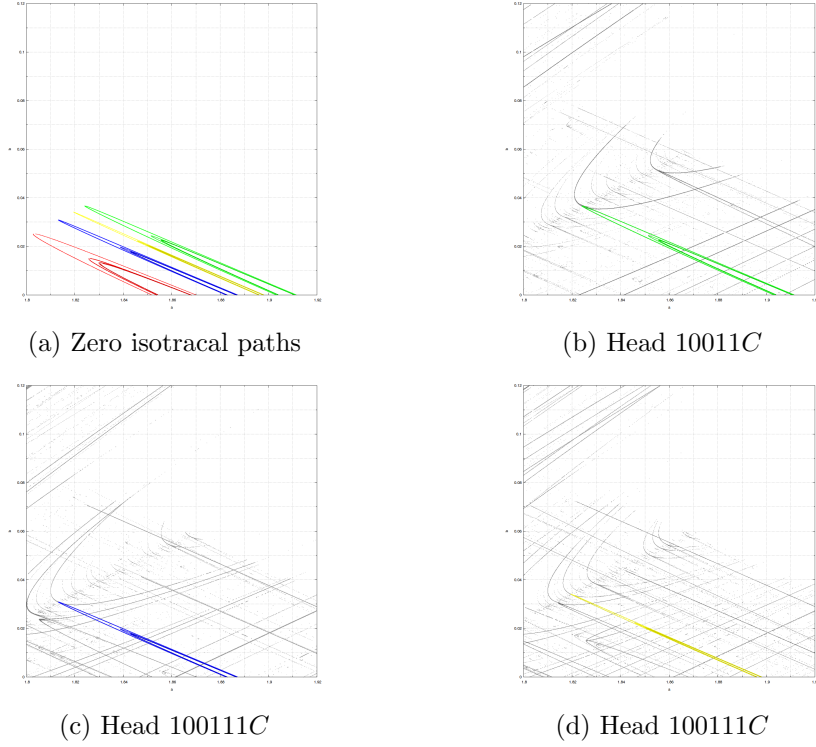


Figure 11: For the Hénon family $F_{a,b}$, in Figure 11a zero isotracal paths are plotted for heads 1001C, 10011C, 100111C and 1001111C. In Figures 10, 11b and 11c the same paths are plotted, for a fixed head, together with scatterplots of parameters with attracting points of the same period.

where ι is some embedding of the set of unimodal maps into the boundary of the space of Hénon-like diffeomorphisms?

and

Question B'. For each positive integer i , let $f_{-,i}$ and $f_{+,i}$ have critical orbits c_-^i and c_+^i of types v_-^i and v_+^i respectively. Let C_-^i and C_+^i denote the corresponding periodic orbits for the degenerate Hénon-like maps $F_{-,i,0}$ and $F_{+,i,0}$ respectively. Does there exist, for each i , a one-parameter family of Hénon-like maps $F_{i,t}$ realising a braid equivalence connecting $(C_-^i, F_{-,i,0})$ and $(C_+^i, F_{+,i,0})$?

References

- [1] Joan S. Birman, Braids, links, and mapping class groups, Princeton University Press, Princeton, N.J., 1974, Annals of Mathematics Studies, No. 82. MR 0375281 (51 #11477)

- [2] Philip Boyland, Braid types and a topological method of proving positive entropy, Boston University, 1984.
- [3] Philip Boyland, Topological methods in surface dynamics, *Topology Appl.* **58** (1994), no. 3, 223–298. MR 1288300 (95h:57016)
- [4] André de Carvalho and Toby Hall, The forcing relation for horseshoe braid types, *Experimental Mathematics* **11** (2002), no. 2, 271–288.
- [5] André de Carvalho, Toby Hall, and Peter Hazard, Braid equivalence in the Hénon family II, in preparation, 2015.
- [6] R. Devaney and Z. Nitecki, Shift automorphisms in the Hénon mapping, *Comm. Math. Phys.* **67** (1979), no. 2, 137–146. MR 539548 (80f:58035)
- [7] Hassan El Hamouly and Christian Mira, Singularités dues au feuilletage du plan des bifurcations d’un difféomorphisme bi-dimensionnel, *C. R. Acad. Sci. Paris Sér. I Math.* **294** (1982), no. 12, 387–390. MR 659728 (83m:58056)
- [8] Toby Hall, The creation of horseshoes, *Nonlinearity* **7** (1994), 861–924.
- [9] Vagn Lundsgaard Hansen, Braids and coverings: selected topics, London Mathematical Society Student Texts, vol. 18, Cambridge University Press, Cambridge, 1989, With appendices by Lars Gæde and Hugh R. Morton. MR 1247697 (94g:57004)
- [10] Philip Holmes, Knotted periodic orbits in suspensions of Smale’s horseshoe: period multiplying and cabled knots, *Phys. D* **21** (1986), no. 1, 7–41. MR 860006 (88b:58112)
- [11] Ittai Kan, Hüseyin Koçak, and James A. Yorke, Antimonotonicity: concurrent creation and annihilation of periodic orbits, *Ann. of Math. (2)* **136** (1992), no. 2, 219–252. MR 1185119 (94c:58135)
- [12] Mikhail Lyubich, The quadratic family as a qualitatively solvable model of chaos, *Notices Amer. Math. Soc.* **47** (2000), no. 9, 1042–1052. MR 1777885 (2001g:37063)
- [13] John Milnor, Remarks on iterated cubic maps, *Experiment. Math.* **1** (1992), no. 1, 5–24. MR 1181083 (94c:58096)
- [14] Jacob Palis, Jr. and Floris Taken, Hyperbolicity & sensitive chaotic dynamics at homoclinic bifurcations, *Cambridge Studies in Advanced Mathematics*, vol. 35, Cambridge University Press, 1993.
- [15] Atsuro Sannami, A topological classification of the periodic orbits of the Henon family, Tech. report, Hokkaido University, 1988.

Table 1: Braid Equivalences in Cyclic Notation.

critical itinerary	cyclic notation
1001010C	2,7,3,5,0,4,6,1
1001110C	2,7,3,0,5,4,6,1
1001010010C	2,7,10,3,8,5,0,4,9,6,1
1001110010C	2,7,10,3,8,0,5,4,9,6,1
1001010010110C	2,7,13,10,3,8,5,0,11,4,9,12,6,1
1001110010110C	2,7,13,10,3,8,0,5,11,4,9,12,6,1
1001010010110110C	2,7,16,13,10,3,8,5,0,14,11,4,9,12,15,6,1
1001110010110110C	2,7,16,13,10,3,8,0,5,14,11,4,9,12,15,6,1
10011110C	2,8,3,0,6,4,5,7,1
10011010C	2,8,3,6,0,4,5,7,1
10011110010C	2,8,11,3,9,0,6,4,5,10,7,1
10011010010C	2,8,11,3,9,6,0,4,5,10,7,1
10011110010110C	2,8,14,11,3,9,0,6,12,4,5,10,13,7,1
10011010010110C	2,8,14,11,3,9,6,0,12,4,5,10,13,7,1
10011010010110110C	2,8,17,14,11,3,9,6,0,15,12,4,5,10,13,16,7,1
10011110010110110C	2,8,17,14,11,3,9,0,6,15,12,4,5,10,13,16,7,1
100111010C	2,9,3,7,0,5,4,6,8,1
100111110C	2,9,3,0,7,5,4,6,8,1
100111010010C	2,9,12,3,10,7,0,5,4,6,11,8,1
100111110010C	2,9,12,3,10,0,7,5,4,6,11,8,1
100111010010110C	2,9,15,12,3,10,7,0,13,5,4,6,11,14,8,1
100111110010110C	2,9,15,12,3,10,0,7,13,5,4,6,11,14,8,1
100111010010110110C	2,9,18,15,12,3,10,7,0,16,13,5,4,6,11,14,17,8,1
100111110010110110C	2,9,18,15,12,3,10,0,7,16,13,5,4,6,11,14,17,8,1
1001111110C	2,10,3,8,0,6,4,5,7,9,1
1001111010C	2,10,3,8,6,0,4,5,7,9,1
1001111110010C	2,10,13,3,11,0,8,6,4,5,7,12,9,1
1001111010010C	2,10,13,3,11,8,0,6,4,5,7,12,9,1
1001111110010110C	2,10,16,13,3,11,0,8,14,6,4,5,7,12,15,9,1
1001111010010110C	2,10,16,13,3,11,8,0,14,6,4,5,7,12,15,9,1
1001111110010110110C	2,10,19,16,13,3,11,0,8,17,14,6,4,5,7,12,15,18,9,1
1001111010010110110C	2,10,19,16,13,3,11,8,0,17,14,6,4,5,7,12,15,18,9,1

Continued on Next Page...

Table

critical itinerary	period	unimodal a	critical itinerary	prefix	decoration
100110010100110C	8	1.85173004941	1001010C	1001	10
100110011100110C	8	1.87000388083	1001110C	1001	10
1001100101001100100110C	11	1.85376146047	1001010010C	1001	10010
1001100111001100100110C	11	1.86808014899	1001110010C	1001	10010
10011001010011001001101100110C	14	1.85420779956	1001010010110C	1001	10010110
10011001110011001001101100110C	14	1.86768154112	1001110010110C	1001	10010110
10011001010011001001101100110C	17	1.85429374549	1001010010110110C	1001	10010110110
10011001110011001001101100110C	17	1.86760846133	1001110010110110C	1001	10010110110
2,11,6,15,3,12,7,9,0,4,13,8,14,5,10,1	9	1.90311677305	10011110C	1001	110
2,11,6,15,3,12,7,0,9,4,13,8,14,5,10,1	9	1.91144463147	10011010C	1001	010
2,11,18,6,15,22,3,12,19,7,16,9,0,4,13,20,8,21,14,5,17,10,1	12	1.90383983136	10011110010C	1001	110010
2,11,18,6,15,22,3,12,19,7,16,0,9,4,13,20,8,21,14,5,17,10,1	12	1.91074213574	10011010010C	1001	010010
2,11,18,6,15,22,3,12,19,7,16,0,9,4,13,20,8,21,14,5,17,10,1	15	1.90396328656	1001111001010C	1001	110010110
2,11,25,18,6,15,29,22,3,12,26,19,7,16,9,0,23,4,13,27,20,8,21,28,14,5,17,24,10,1	15	1.91062464072	1001101001010C	1001	010010110
2,11,25,18,6,15,29,22,3,12,26,19,7,16,0,9,23,4,13,27,20,8,21,28,14,5,17,24,10,1	18	1.90398296779	10011010010110110C	1001	010010110110
2,11,32,25,18,6,15,36,29,22,3,12,33,26,19,7,16,9,0,30,23,4,13,34,27,20,8,21,28,35,14,5,17,24,31,10,1	18	1.91060625301	10011110010110110C	1001	110010110110
2,11,32,25,18,6,15,36,29,22,3,12,33,26,19,7,16,0,9,30,23,4,13,34,27,20,8,21,28,35,14,5,17,24,31,10,1	10	1.88240793375	10011010C	1001	1010
	10	1.88717220640	100111110C	1001	1110

Table 2: Braid Equivalences and Associated Data.

head	period	unimodal a	critical itinerary	prefix	decoration
1001C	8	1.85173004941	1001010C	1001	10
	8	1.87000388083	1001110C	1001	10
	11	1.85376146047	1001010010C	1001	10010
	11	1.86808014899	1001110010C	1001	10010
	14	1.85420779956	1001010010110C	1001	10010110
	14	1.86768154112	1001110010110C	1001	10010110
	17	1.85429374549	1001010010110110C	1001	10010110110
	17	1.86760846133	1001110010110110C	1001	10010110110
10011C	9	1.90311677305	10011110C	1001	110
	9	1.91144463147	10011010C	1001	010
	12	1.90383983136	10011110010C	1001	110010
	12	1.91074213574	10011010010C	1001	010010
	15	1.90396328656	1001111001010C	1001	110010110
	15	1.91062464072	1001101001010C	1001	010010110
	18	1.90398296779	10011010010110110C	1001	010010110110
	18	1.91060625301	10011110010110110C	1001	110010110110
100111C	10	1.88240793375	10011010C	1001	1010
	10	1.88717220640	100111110C	1001	1110

Continued on Next Page...

Table 2 – Continued

head	period	unimodal a	critical itinerary	prefix	decoration
1001111C	13	1.88286957759	100111010010C	1001	1010010
	13	1.88672860609	100111110010C	1001	1110010
	16	1.88295631360	10011010010110C	1001	1010010110
	16	1.88664609851	100111110010110C	1001	1110010110
	19	1.88297117918	10011010010110110C	1001	1010010110110
	19	1.88663211208	100111110010110110C	1001	1110010110110
10011001C	11	1.89575422001	1001111110C	1001	11110
	11	1.89808902792	1001111010C	1001	11010
	14	1.89596323393	100111110010C	1001	11110010
	14	1.89787945132	1001111010010C	1001	11010010
	17	1.89600029216	100111110010110C	1001	11110010110
	17	1.89784256570	1001111010010110C	1001	11010010110
	20	1.89600636282	100111110010110110C	1001	11110010110110
	20	1.89783655715	1001111010010110110C	1001	11010010110110
	16	1.93213488504	100110010100110C	10011001	100110
	16	1.93235574679	100110011100110C	10011001	100110
10011001C	23	1.93213896428	1001100101001100100110C	10011001	1001100100110
	23	1.93235156026	1001100111001100100110C	10011001	1001100100110
	30	1.93213911573	10011001010011001001101100110C	10011001	10011001001101100110
	30	1.93235140816	10011001110011001001101100110C	10011001	10011001001101100110
	37	1.93213912112	100110010100110010011011001101100110C	10011001	100110010011011001101100110
	37	1.93235140286	100110011100110010011011001101100110C	10011001	100110010011011001101100110